AN INTRODUCTION TO A NEW CONCEPT: THE DYNAMIC STABILITY OF DISKS FREELY DESCENDING IN A FLUID MEDIA

by

BILLY LEE HIMES, SR.

B. S., Kansas State University of
Agriculture and Applied Science, 1958

A THESIS

submitted in partial fulfillment of the

requirements for the degree

MASTER OF SCIENCE

Department of Chemical Engineering

KANSAS STATE UNIVERSITY
OF AGRICULTURE AND APPLIED SCIENCE

1960

TABLE OF CONTENTS

INTRODUCTION

A Definition of Dynamic Stability

In the beginning of time on this earth unstability in motion was observable when the first leaf fell from the first plant. As the leaf descended toward the earth it either fluttered, oscillated, revolved, spiraled, or combined all or part of these motions in its erratic descent. This erratic behavior was indicative of the non-uniform velocity of the leaf along a vertical to the earth. Therefore it was exhibiting unstable motion, or dynamic unstability.

If the first man had been able to measure the height of the leaf at equal increments of time, dynamic stability might have been acknowledged millions of years ago. Initially the first man might have noticed that the measured heights of the leaf did not decrease the same amount over each equal increment of time. This indicated non-uniform velocity in the vertical direction. The first man might then have compared these measured heights with the comparable heights of a leaf imagined as descending toward the earth with uniform velocity in the vertical direction. From comparing each actual height with each imagined height for the same time of descent he would have found a difference. By then calculating the mean of the summation of these absolute differences he might have called the resultant value dynamic unstability. However, he didn't. Dynamic unstability had always existed, but it was necessary for man to measure it to verify its existence.

Simply, dynamic unstability was the mean deviation of the actual path of the leaf from some imaginary path, described in this study by a least squares line through the actual path. For this imaginary path no assumptions were made as to the uniformity of the leaf's velocity vectors horizontal to the earth's surface. It was possible for the leaf to follow a curvelinear path in its actual descent and exhibit no dynamic unstability as long as it descended equal increments of vertical distance in equal increments of universal time.

The difference, or deviation, of the actual path from an imaginary path had units of length. Therefore, dynamic unstability had units of length. As the phraseology might indicate, dynamic stability was defined as the reciprocal, or opposite, of dynamic unstability. Therefore, its units were reciprocal length. In order to adequately describe the meaning of dynamic stability it was necessary to define it in mathematical terms; this was presented in the Mathematical Definition of Dynamic Stability.

Many investigators, including Wadell (8), Pettyjohn (6), Squires (7), Wetherall (9), and Becker (1), had observed this behavior in most describable sizes and shapes of particles, but carried the investigation little further than recording these observations and, in some cases, comparing them with conventional concepts of particle behavior in fluids. No attempt had been made to numerically evaluate or to define the unstability of movement of particles in fluids.

Disks which exhibit infinite stability are illustrated in PLATE I. They were defined as a stationary disk, floating on the surface of a fluid, with no velocity vector and as a moving disk, descending or ascending in the fluid, with velocity but no acceleration. Conversely, infinite unstability was postulated as the motion of a disk which exhibited constant acceleration through infinite time. A disk accelerating and decelerating through finite time had a finite value of dynamic stability and unstability. It was these latter descents of free-falling disks with which this study was concerned.

Even as the best measurement is no better than an approximation of the true value, so no motion is absolutely dynamically stable. Due to limitations on man's ability to measure minute differences, it is possible to measure and subsequently calculate a descent as dynamically stable, although theoretically a dynamically stable descent is unobtainable. As man's abilities to measure improve that which was previously classified as dynamically stable may no longer be so classified.

Objectives of Study

The original objectives of this study were:

1) To continue work initiated by Professor R. C. Hall* and to refine the mathematical definition of the concept of free-falling particle behavior in an infinite expanse of fluid.
2) To calculate numerical values of stability from actual descents of disks of varying properties.

Later objectives were:

3) To observe and define the types of motion of free-falling disks in a fluid media.
4) To correlate these values of dynamic stability with the types of motion observed.

Objectives 3) and 4) were planned after an initial study of the types of motions of disks had shown that some of the disks consistently fell in the same manner.

*Private communications

Review of Literature

A literature search revealed that dynamic stability had aroused the curiosity of many investigators, but that this effort was apparently the first actually measuring it. The literature search included the following material:

1. Chemical Abstracts dating back to 1930.
2. Physics Abstracts back to 1950.
3. All theses and abstracts of theses located in the Kansas State University Library.
4. Numerous more recent publications not yet abstracted.

No experimentation resembling dynamic stability studies was uncovered. However, several articles discussing the appearance of motion in particles descending through a fluid media were available.

From an article by Wadell (8), the following was quoted:

> Franz Schulze stated that the translation velocity of a flat stone in air or water depends upon its position in respect to the direction of translation. Jordan noted that mineral particles readily took a position with their broad side at right angles to the direction of fall. Schmiedel found that thin disks at very low Re showed no tendency to take any particular settling position while at higher Re the disks tended toward a horizontal position regardless of the position at the start. At still higher Re's periodic oscillations set in and the settling took place in a zig-zag path.

On the study of spheres, octahedrons, cubes, and tetrahedrons Pettyjohn and Christiansen (6), stated:

> Wheras in the streamline flow range ($Re < 0.05$) the particles did not favor any particular orientation with respect to the direction of motion, at $Re \sim 10$, the tetrahedrons and cubes assumed an orientation with a face in the horizontal plane or perpendicular to the direction of motion and the other particles showed a tendency to do likewise by $Re \sim 20$. This orientation was maintained up to $Re = 70$ to 300 where the particles beginning with the tetrahedrons, 'teetered' or

wobbled and sventually spun or rollsd on a horizontal axis and followed a spiral path rather than a straight vsrtical path in thsir descent.

From an articls on ths ssdimsntation of thin disks by Squires and Squires (7), it was stated tbat at very low Reynolds numbsrs, in ths viscous region a body, sucb as a disk, possssing three perpendicular planes has no tsndency to assums any particular orientation during fall. It was further statsd:

> A disc placed with its flat facs parallsl to the dirsction of motion of ths fluid will maintain this orientation. At higbsr Reynolds numbers, in the turbulent region, the eddiss sst up by the motion of tbe disc througb tbe fluid act to maintain the particle at right angles to the direction of motion. Tberefore, a disc will always ssttle in a horizontal position in the turbulent rsgion, and its position when in ths viscous rsgion will dspend upon its initial inclination.

Miyagi (5), discussed ths motion of an air bubble rising in watsr. Ths course of ths bubble was three-dimensional; it was obssrvsd to bs a belix around a vertical. Tbs major axis of ths bubble was always psrpendicular to its course. PLATE XVIII, Fig. 1, bassd on Fig. 12 of Miyagi's articls illustrated tbs riss of an air bubbls in only two of tbe thres dimensions.

Wsthsrall (9), was able to photograph the track of a flat solid (a small crystal of A_gNO_3) as it descended in acidulatsd water. PLATE XVIII, Fig. 2, was based on this photograpb.

Bscker (1), providsd tbs following information in a table on tbe insrtial drag characteristics of freely oriented bluff bodiss. At Rs's of 0.1 - 5.5 it was statsd tbat all orientations wers stable wben there were thrse or more perpsndicular axss of symmetry in tbe dsscsnding disk. At Re's of 5.5 - 200 the motion was stable in the position of maximum drag. For Rs's of 200 - 500 tbe motion was unpredictable.

Disks tended to wobble, while fuller bluff bodies tended to rotate.

Considering the results of this literature search it was apparent that this study initiated by Professor R. C. Hall of Kansas State University in 1955 was the first recognition of dynamic stability as a property of particles in an infinite expanse of fluid.

Illustration of Definition of Dynamic Stability

The following diagram, PLATE I, illustrates the two possible manners in which a disk could theoretically exhibit complete dynamic stability.

EXPLANATION OF PLATE I

Illustration of infinitely stable motion of disks,

where $\psi' =$ dynamic unstability $= 0$,

$\psi =$ dynamic stability $= \infty$, and

$U =$ velocity.

PLATE I

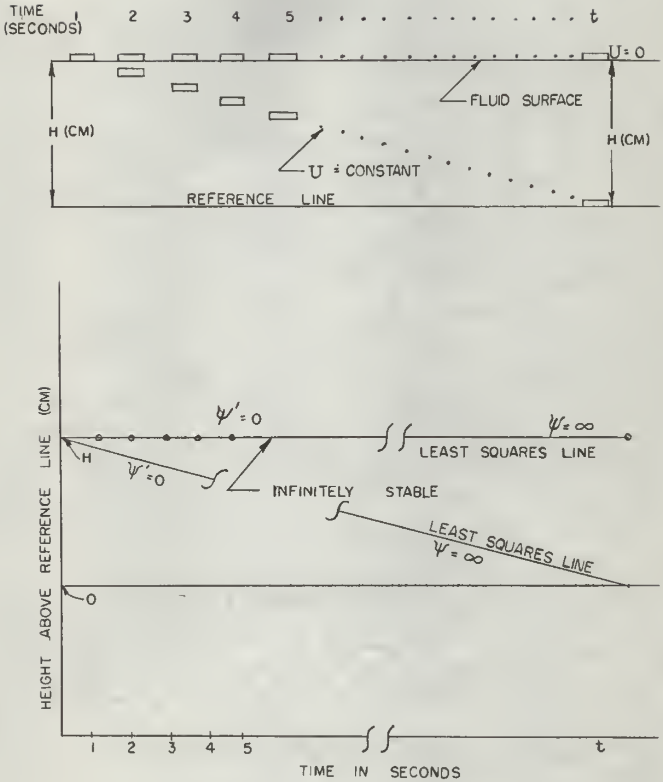
TIME (SECONDS)
1 2 3 4 5 t
U = 0
FLUID SURFACE
H (CM)
U ≐ CONSTANT
H (CM)
REFERENCE LINE
HEIGHT ABOVE REFERENCE LINE (CM)
ψ′ = 0
ψ = ∞
H
LEAST SQUARES LINE
ψ′ = 0
INFINITELY STABLE
LEAST SQUARES LINE
ψ = ∞
O
1 2 3 4 5 t
TIME IN SECONDS

PROCEDURE OF MEASUREMENTS

Outline of Procedure

For the study a series of 46 dieke, approximately one inch in diameter and a quarter inch thick, were conetructed. Diek 1 wae lucite. Disks 2 through 26 had cores of stainlees steel and rims of lucite. Disk 27 was all etainleee eteel. Disks 28 through 46 had lucite coree and stainlees steel rims. By varying the eize of the coree the diske were each given different weights and momente of inertia. Only part of the disks were used, due to the deterioration of the rest.

The procedure was to drop each disk in turn through a liquid, take motion picturee of the descent, and measure on a projection of each frame of the movie the diek's relative height above a bottom reference line (PLATE XII).

Detailed Procedure

The procedure utilized in taking the movies of the disk's deecent in a liquid media required the eervices of aesistante A and B and photographer P (PLATES II, III, and IV). For the descent of each disk the prooedure was as follows:

1.) As assistant B changed the cards designating the disk number, the drop number, and the liquid temperature, assistant A placed the dasignated disk on the particle vacuum release mechanism performing operations 1, 2, and 3 (PLATE V).

2.) B then turned on the foreground lights illuminating the information cards. Thie signaled P to photograph thie information.

3). Having built up, during a twenty second count, sufficient vacuum to hold the diek the line from the vacuum pump was closed and 'bled' by A in performing operatione 4 and 5 (PLATE V). The release mechaniem holding the disk wae then lowered into the liquid.

4.) At the end of fifty-five seconds of a eecond count, A notified B to signal P by means of a buzzer to commence photographing. At sixty eeconde the remaining vacuum wae released by performance of operation 6 (PLATE V), thus allowing the disk to start ite deecent through the liquid.

5.) Ae the particle reached the bottom of the column, B eignaled the photographer to ceaee operation.

6.) This procedure wae repeated for euccessive diske.

An approximately identical method of releaee for the dieke wae obtained by meane of the particle vacuum release mechanism. By allowing a time lapse, the twenty and eixty second counte, and by floating Agile plaetic stars (See Table of Definitions, Appendix) on the fluid eurface, the internal fluid agitation was minimized to a satiefactory degree.

Following the development of the film, measuremente on the descent of the diek were etarted. For this operation aseietants A and B were again utilized. The aesietante were selected on the baeis of the similarity between their meaeurements over several triale. Thie likenees in obeervation of the meaeured quantity allowed the aesietante to be rotated between jobe within any eet of measuremente. To further minimize fatigue and monotony a third assistant C was used when available.

The film was threaded through a special adaptor (PLATE XI) on the projector. The use of this adaptor largely prevented the film from shifting or buckling, as well as adapting the 16mm. film to a 35mm. projector. Prior to starting the measurements the projector was allowed to run twenty to thirty minutes, thus allowing distortion caused by heat from the projection lamp to reach near equilibrium in the film. The focus on the projector was earlier set at an optimum position; this was determined by repeated adjustments of the focus until both assistants were visually satisfied.

The actual measuring operation was in general performed as follows:

1.) After the projector was allowed to heat for twenty to thirty minutes before the day's run, the disk number, liquid temperature, and drop number were identified by assistant B from an identification frame (PLATE XII, Fig. 1) and called to assistant A to be recorded.

2.) The film was then pulled through the projector by assistant A until the frame was found showing the disk to be located just below the top reference line. This frame was the first to be measured for each disk descent.

3.) At this point necessary minor adjustments were made in the frame location on the screen. By means of the turnbuckles and the focus on the projector (PLATE VI and VII) the projected picture of the frame was restricted between vertical boundary lines drawn on the screen (PLATE VIV). By pulling the film up or down the image of the top reference line was placed in approximate line with a reference mark drawn on the screen (PLATE VIV). These adjustments minimized any possible error in measurements. These errors occurred from minute differences between each frame's position in the projector due to the slight bending of the film and the minor deviations of the film from the vertical in passing each frame through the adapter (PLATE XI).

4.) After these preliminaries were finished the readings on a frame were started. By means of a target (PLATES VI, IX, and X), B located the bottom reference line, the particle, and the top reference line positions, respectively. These locations were in turn transmitted by a system of pulleys to a stationary measuring device (PLATE VI and VIII) where the values L_H, L_P, and L_L were read and recorded by A. For reasons of uniformity in the tension on the pulley wire the target was always <u>adjusted</u> <u>downward</u> onto the image being measured. For statistical reasons the readings were repeated six times for each frame. For each reading, by means of a signal light, B notified A when the target was set and by means of a buzzer, A notified B when he had completed the reading (PLATE VIII).

5.) After completing this first frame a second frame was placed in position. For each frame, after the initial frame of a day's measurements, a ten to fifteen second time lapse was allowed so that the frame had sufficient time to reach equilibrium with the distortions caused by the heat of the projection lamp striking the film.

6.) The same procedure was employed for each frame. The measurements for any one disk were terminated at the frame showing the particle in its final position above the bottom reference line.

By utilization of a true length correction factor for each frame, $\frac{100}{L_P - L_L}$, changes in the film due to moderate temperature and humidity changes were prevented from causing measuring errors. More rapid distortion due to extreme temperature changes in the film as caused by the heat from the projection lamp were minimized by short time lapses between each frame read in which equilibrium was reached in the film. Fatigue in the measuring personnel was minimized by changes in duties every half hour to one hour, depending on the weather and by taking frequent rest breaks.

Errors in measurement caused by shifts in the picture projection due to extraneous disturbances were avoided by the replacement of such data after the disturbance had ceased. Minor disturbancee and vibrations were alleviated by the location of rubber padding under the projector platform and by the use of several restraining wires around the projector (PLATE VI and VIII).

Diagrams of Equipment

The following pages present diagrams of the experimental equipment and illustrate procedures.

EXPLANATION OF PLATE II

Front view of particle drop column showing lighting arrangement and personnel placement for photography of disk descent in liquid column.

PLATE II

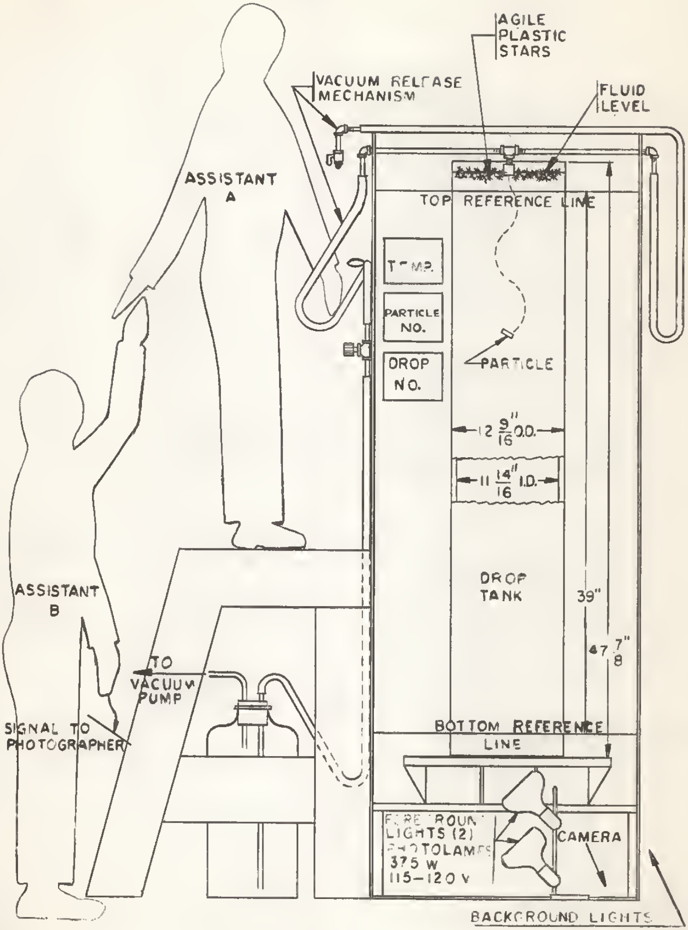
AGILE
PLASTIC
STARS
VACUUM RELEASE
MECHANISM
FLUID
LEVEL
ASSISTANT
A
TOP REFERENCE LINE
TEMP.
PARTICLE
NO.
DROP
NO.
PARTICLE
12 9/16" O.D.
11 14/16" I.D.
DROP
TANK
39"
47 7/8"
ASSISTANT
B
TO
VACUUM
PUMP
SIGNAL TO
PHOTOGRAPHER
BOTTOM REFERENCE
LINE
LIGHTS (2)
375 W
115-120 V
CAMERA
BACKGROUND LIGHTS

EXPLANATION OF PLATE III

Top view of particle drop column showing personnel, lighting and camera positions for photography of disk descent in fluid media.

PLATE III

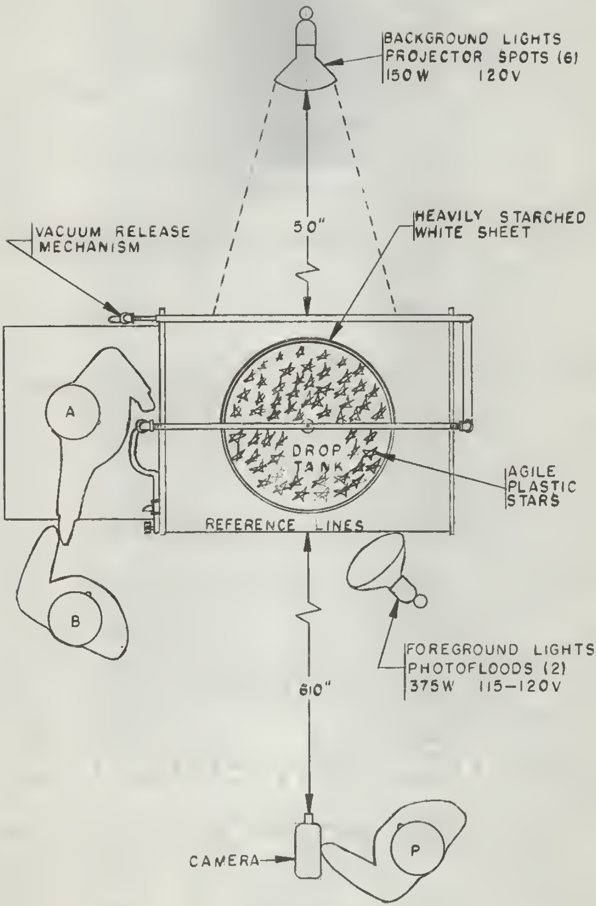
BACKGROUND LIGHTS
PROJECTOR SPOTS (6)
150 W 120 V
50"
VACUUM RELEASE
MECHANISM
HEAVILY STARCHED
WHITE SHEET
A
DROP
TANK
AGILE
PLASTIC
STARS
REFERENCE LINES
B
FOREGROUND LIGHTS
PHOTOFLOODS (2)
375 W 115-120 V
610"
CAMERA
P

EXPLANATION OF PLATE IV

Schematic of arrangement for photography of disk descent in fluid media in glass column. ////// heavily starched white sheet as background of drop tank.

PLATE IV

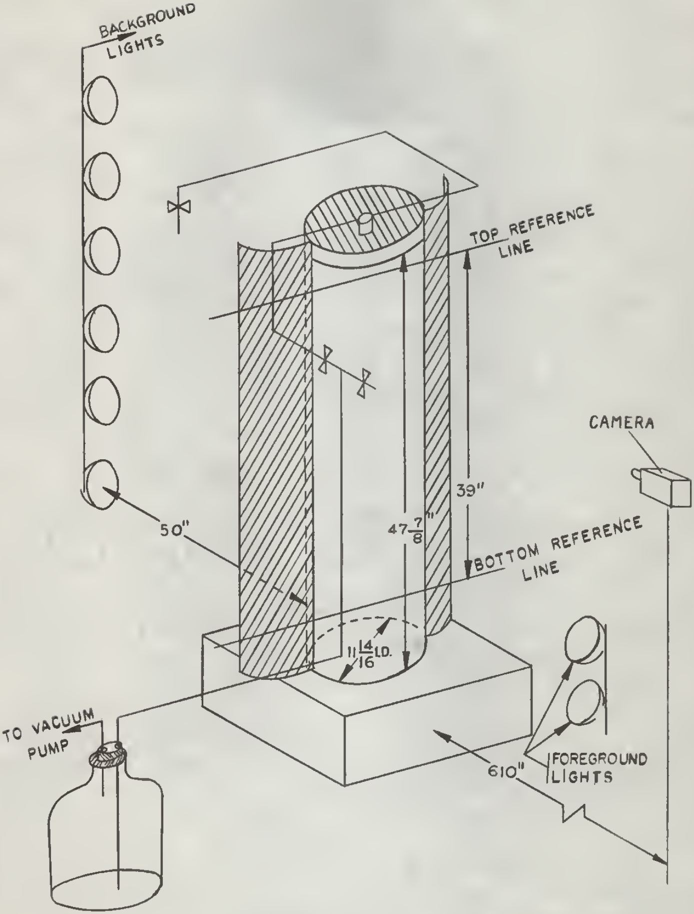
BACKGROUND
LIGHTS
TOP REFERENCE
LINE
CAMERA
39"
50"
$47\frac{7}{8}$"
BOTTOM REFERENCE
LINE
$11\frac{14}{16}$ I.D.
TO VACUUM
PUMP
610"
FOREGROUND
LIGHTS

EXPLANATION OF PLATE V

Schematic of particle vacuum drop mechanism giving order of operation of valves in actual release of disk in fluid media.

PLATE V

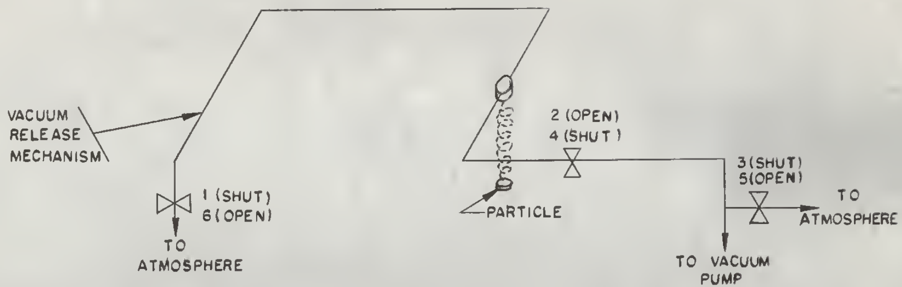
VACUUM
RELEASE
MECHANISM
1 (SHUT)
6 (OPEN)
TO
ATMOSPHERE
PARTICLE
2 (OPEN)
4 (SHUT)
3 (SHUT)
5 (OPEN)
TO
ATMOSPHERE
TO VACUUM
PUMP

EXPLANATION OF PLATE VI

Side view of personnel and equipment for measuring L_L, L_P, and L_H on film taken in PLATES II, III, IV, and V. Shows placement of projector, reading device, dark room, and screen.

PLATE VI

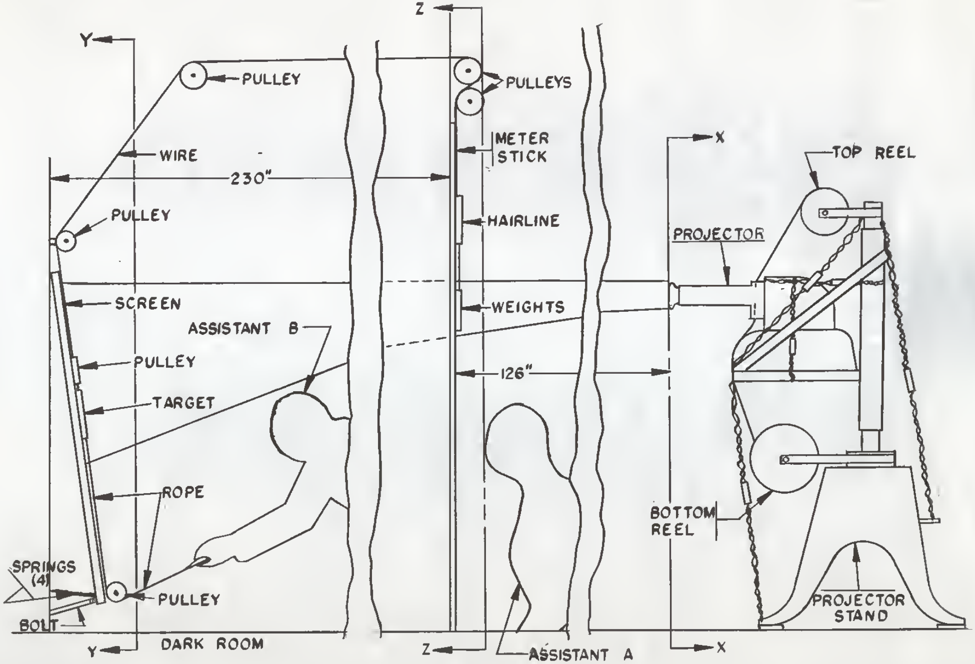

Y
Y
PULLEY
WIRE
230"
PULLEY
SCREEN
ASSISTANT B
PULLEY
TARGET
ROPE
SPRINGS (4)
BOLT
PULLEY
DARK ROOM
Z
Z
PULLEYS
METER STICK
HAIRLINE
WEIGHTS
126"
ASSISTANT A
X
X
TOP REEL
PROJECTOR
BOTTOM REEL
PROJECTOR STAND

EXPLANATION OF PLATE VII

Front view of projector showing location of turnbuckles for right and left adjustments of film projection and focus for refinement and right and left cant of projection.

PLATE VII

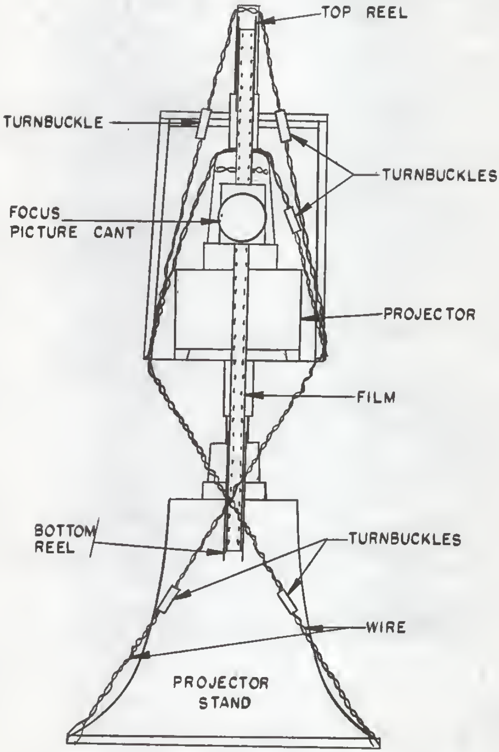

VIEW X-X

EXPLANATION OF PLATE VIII

Front view of measuring device showing assistant A, projectionist and reader-recorder of L_L, L_P, and $L_{H'}$ values.

PLATE VIII

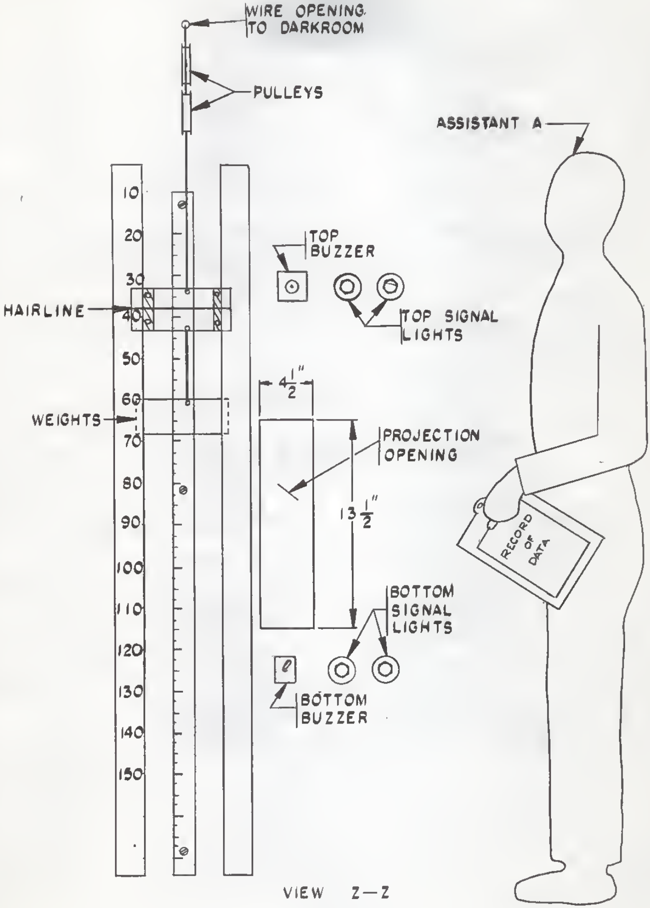

VIEW Z—Z

EXPLANATION OF PLATE IX

Front view of screen showing location of picture, target, and assistant B - target adjuster.

PLATE IX

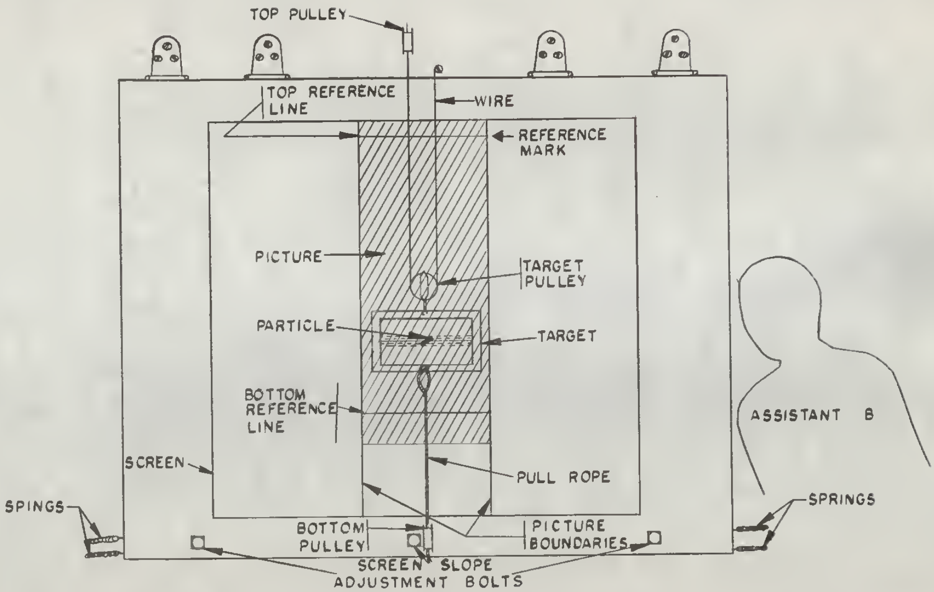

VIEW Y—Y

EXPLANATION OF PLATE X

Front view of target, showing actual application of target to three measured elements of each frame.

PLATE X

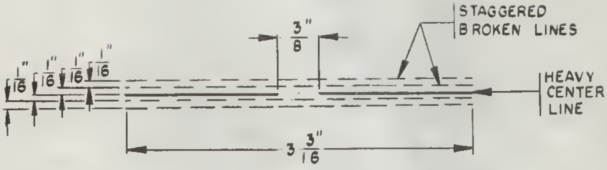

TARGET

LOCATION OF TOP REFERENCE LINE ON TARGET

LOCATION OF BOTTOM REFERENCE LINE ON TARGET

LOCATION OF PARTICLE ON TARGET

OPERATION OF TARGET

EXPLANATION OF PLATE XI

Front and side views of adapter
of 16mm film to 35mm projector.

PLATE XI

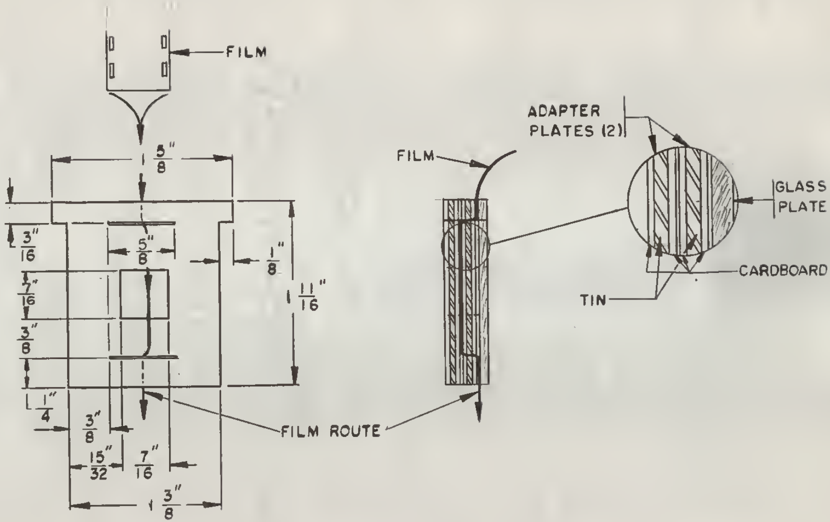

ADAPTER PLATE

EXPLANATION OF PLATE XII

Frames from movie of the descent of a disk.

Fig. 1. Identification frame.

//// temperature of fluid media

\\\\ disk number

≡ drop number

Fig. 2. Measuring frame.

L_H = top reference line

L_P = disk

L_L = bottom reference line

PLATE XII

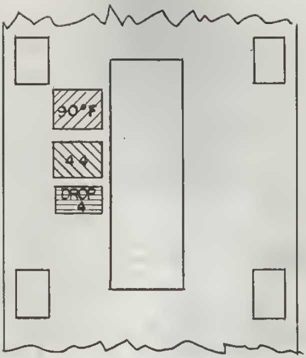

Fig. 1

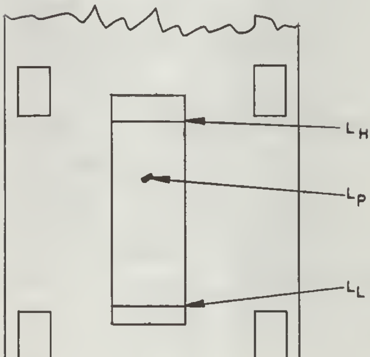

Fig. 2

MATHEMATICAL DEFINITION OF DYNAMIC STABILITY

Initial Calculatione on Data from Repreeeentative Frame of a Descent

DATE 7-17-59 PARTICLE No. 2

θ		L_H	L_P	L_L	θ
1	1	105.23	104.52	25.52	
	2	105.22	104.56	25.51	
	3	105.21	104.52	25.49	
	4	105.20	104.52	25.50	
	5	105.18	104.48	25.49	
	6	105.18	104.49	25.51	
	AVE	105.20	104.52	25.50	
	L_H-L_L	79.70	L_P-L_L	79.01	
	T.L.	1.25470	h_i	99.14	
2	1	102.51	99.38	22.72	
	2	102.51	99.32	22.71	
	3	102.49	99.30	22.71	
	4	102.49	99.34	22.71	
	5	102.47	99.32	22.68	
	6	102.50	99.31	22.68	
	AVE.	102.50	99.33	22.70	
	L_H-L_L	79.80	L_P-L_L	76.63	
	T.L.	1.25313	h_i	96.03	
	1	102.91	96.88	23.29	
	2	102.89	96.90	23.30	

θ = frame number.

L_H = meaeured height of top reference line, relative to base line.

L_P = meaeured height of diek, relative to baee line.

L_L = measured height of bottom reference line, relative to baee line.

T.L. = $\frac{100}{L_H - L_L}$ = faotor for adjueting relative valuee to true values.

$$h_i = (L_P - L_L)\left(\frac{100}{L_H - L_L}\right) = \text{true height of disk above bottom reference line.}$$

(See PLATE XIII, Fig. 1 for physical descriptions of L_H, L_P, and L_L).

For first reading on first frame:

θ	Reading	L_H	L_P	L_L
1	1	105.23	104.52	25.52

$$L_H - L_L = 79.71$$

$$L_P - L_L = 79.00$$

$$T.\ L. = \frac{100}{L_H - L_L} = 1.25455$$

$$h_i = (L_P - L_L)\ (T.L.) = 99.11$$

For readings 2, 3, 4, 5, 6 on frame one - above procedure repeated.

Then:

$$h_{i_1} = 99.11$$
$$h_{i_2} = 99.17$$
$$h_{i_3} = 99.13 \qquad h_{i_{avg.}} = 99.14 = h_{\bar{i}}$$
$$h_{i_4} = 99.15$$
$$h_{i_5} = 99.12$$
$$h_{i_6} = 99.13$$

Calculation of 90% confidence interval on $h_{\bar{i}}$ of frame one:

n	$(h_{i_n} - h_{\bar{i}})$	$(h_{i_n} - h_{\bar{i}})^2$
1	-0.03	0.0009
2	+0.03	0.0009
3	-0.01	0.0001
4	+0.01	0.0001
5	-0.02	0.0004
6	+0.01	0.0001

$$\sum (h_{i_n} - h_{\bar{i}})^2 = 0.0025$$

$$S_i^2\,(h_i) = \frac{\sum (h_{i_n} - \bar{h}_i)^2}{n - 1} = \frac{0.0025}{5} = 0.0005$$

$$S^2 = \frac{\sum (h_{i_n} - \bar{h}_i)^2}{n(n-1)} = \frac{0.0005}{6} = 0.000083$$

$$S = \sqrt{S^2} = \sqrt{0.000083} = 0.0091$$

$t_{0.05}$ = Student's t for 95% confidence interval = 2.571

$$(t_{0.05})\,(s) = 2.571\,(0.0091) = 0.0234$$

$$h_{i_{t_{0.05}}} = 99.14 \pm 0.02$$

$$99.12 \leqq \bar{h}_i \leqq 99.16$$

The confidence intervals on the measurements provided a means of detecting errors that occurred at any time during the processing of the data.

Least squares line (sample regression line):

Observation Number	θ	h_{i_θ}	θ^2	θh_{i_θ}
1	1	99.14	1	99.14
2	2	96.03	4	192.06
.	.	.	.	.
.	.	.	.	.
.	.	.	.	.
.	.	.	.	.
θ	.	.	.	.
	$\overline{\sum\theta}$	$\overline{\sum h_{i_\theta}}$	$\overline{\sum\theta^2}$	$\overline{\sum\theta h_{i_\theta}}$

$$(\text{Number of observations})\ k + (\sum\theta)\,j = \sum h_{i_\theta}$$

$$(\sum\theta)\ k + (\sum\theta^2)\ j = \sum\theta h_{i_\theta}$$

Solve simultaneous equations for k and j.

Equation of least squares line:

$$y = k + jx$$

k = y intercept at $\theta = 0$

j = slope of least squares line, or sample regression coefficient

Definition of Dynamic Stability, $\psi s^2_{y.x}$ and $\psi\sqrt{s^2_{y.x}}$

At any frame, θ, the absolute deviation from regression of the height of a disk from the height of the least squares line through its path $= h_{i_\theta} - (k + \theta j)$, where

h_{i_θ} = the height of the disk at θ,

and $k + \theta j$ = the height of the least squares line at θ.

Assumption: Each frame over the descent of a disk was equal to the same increment of universal time, where the conversion factor of frames to seconds was F.

For any randomly selected descent of a disk consisting of Θ frames, the summation of the squares of absolute deviation from regression =

$\left|h_{i_1} - (k + j)\right|^2$ times (number of frames having this absolute deviation, which was always one) times

$(F) + \left|h_{i_2} - (k + 2j)\right|^2 (1) (F) + \ldots\ldots\ldots\ldots$

$\ldots\ldots + \left|h_{i_\theta} - (k + \theta j)\right|^2 (1) (F).$

Units:

$\left|h_{i_1} - (k + \theta j)\right|^2 = cm^2.$

number of frames having above absolute deviation = frames.

$F = \frac{\text{seconds}}{\text{frames}}$

$$cm.^2 \quad \cancel{\text{frame}} \quad \frac{\text{seconds}}{\cancel{\text{frames}}} \quad = cm.^2 \text{ sseconds}$$

Thersfors:

Summation of absoluts dsviations from regression =

$$\left|h_{i_\theta} - (k + \theta j)\right|^2 \quad (1)(F) = F\sum\left|d_{y.x}\right|^2.$$

Finally:

$$\psi' s^2_{y.x} = F\sum\left|d_{y.x}\right|^2 / (\theta - 2)(F)$$

= msan square deviation from regrsssion, or

$$\text{dynamic unstability} = \frac{cm.^2 \text{ seconds}}{\text{frames} \quad \frac{\text{seconds}}{\text{frames}}}$$

$$= cm.^2$$

$\theta - 2$ = total number of frames minus two, sincs two degrees of freedom were lost in ths calculation.

$$\text{Dynamic stability} = \psi s^2_{y.x} = \frac{1}{\psi' s^2_{y.x}} = \frac{1}{cm.^2}$$

$$\text{Or, dynamic stability} = \psi\sqrt{s^2_{y.x}} = \sqrt{\psi s^2_{y.x}} = \frac{1}{cm.}$$

Dsfinition of Dynamic Stability, ψ_{AREA}

(Sse PLATE XIV, Fig. 1, whsrs the shaded area on this plot represents $\psi'_{\text{Area}_\theta}$.)

Trapszoidal Ruls:

(Sss PLATE XIV, Fig. 2 and 3)

$$ab = \left|h_{i_\theta} - (k + \theta j)\right|$$

$$cd = \left|h_{i_{\theta+1}} - \left[k + (\theta + 1)j\right]\right|$$

$$ef = \left|h_{i_{\theta+2}} - \left[k + (\theta + 2)j\right]\right|$$

$$gh = \left|h_{i_{\theta+3}} - \left[k + (\theta + 3)j\right]\right|$$

On Fig. 3:

$$\frac{ab + cd}{2} = wy = xz$$

Area wyzx = area abdc

$$yz = wx = (1)\ F = \text{frames} \ \frac{\text{seconds}}{\text{framss}} = \text{sseconds}$$

$$\text{Area abdfhgeca} = \Psi'\text{Area} = \frac{ab + cd}{2}(1)(F) + \frac{cd + ef}{2}(1)(F)$$
$$+ \frac{ef + gh}{2}(1)(F) = \left(\frac{ab}{2} + cd + ef + \frac{gh}{2}\right) F.$$

Where the experimental curve croesee the leaet equaree curve between coneecutive poeitione of the diek a value C muet be calculated. (See PLATE XIV, Fig. 4)

$$\text{Area a'b'c'd'a'} \quad \frac{\left\{\left|h_{i_\theta} - (k + \theta j)\right|^2 + \left|h_{i_{\theta + 1}} - \left[k + (\theta + 1)j\right]\right|^2\right\}}{2\left\{\left|h_{i_\theta} - (k + \theta j)\right| + \left|h_{i_{\theta + 1}} - \left[k + (\theta + 1)j\right]\right|\right\}} F = C$$

Situation 1. (See PLATE XIII, Fig. 2)

$$\text{Area} = \text{Area a12345678b}$$
$$= \left\{\frac{\left|h_{i_1} - (k + j)\right|}{2} + \left|h_{i_2} - (k + 2j)\right| + \left|h_{i_3} - (k + 3j)\right|\right.$$
$$+ \left|h_{i_5} - (k + 5j)\right| + \frac{\left|h_{i_6} - (k + 6j)\right|}{2} + C_{67}$$
$$\left. + \frac{\left|h_{i_7} - (k + 7j)\right|}{2} + \frac{\left|h_{i_8} - (k + 8j)\right|}{2}\right\}(F)$$

Situation 2. (See PLATE XIII, Fig. 3)

$$\text{Area} = \text{Area a12345678b}$$
$$= \left\{\frac{\left|h_{i_1} - (k + j)\right|}{2} + \left|h_{i_2} - (k + 2j)\right| + \frac{\left|h_{i_3} - (k + 3j)\right|}{2}\right.$$
$$+ C_{34} + \frac{\left|h_{i_4} - (k + 4j)\right|}{2} + \frac{\left|h_{i_5} - (k + 5j)\right|}{2}$$
$$\left. + C_{56} + C_{67} + \frac{\left|h_{i_7} - (k + 7j)\right|}{2} + \frac{\left|h_{i_8} - (k + 8j)\right|}{2}\right\} F$$

Situation 3. (See PLATE XIII, Fig. 4)

$$\text{Area} = \text{Area a}123456789\text{b}$$

$$= \left\{ \frac{\left|h_{i_1} - (k + j)\right|}{2} + \left|h_{i_2} - (k + 2j)\right| + \left|h_{i_3} - (k + 3j)\right| \right.$$

$$+ \left|h_{i_4} - (k + 4j)\right| + \left|h_{i_5} - (k + 5j)\right| + \left|h_{i_6} - (k + 6j)\right|$$

$$\left. + \left|h_{i_7} - (k + 7j)\right| + \left|h_{i_8} - (k + 8j)\right| + \frac{\left|h_{i_9} - (k + 9j)\right|}{2} \right\} (F),$$

where terms 4 and 7 are zero.

In summary:

Area

$$\frac{\text{AREA}_\theta}{(\theta-2)\ F} = \frac{(\text{cm.})\ (\cancel{\text{frames}})\ \frac{\cancel{\text{seconds}}}{\cancel{\text{frame}}}}{(\cancel{\text{frames}})\ \frac{\cancel{\text{seconds}}}{\cancel{\text{frame}}}} = \text{cm.},$$

where F cancels the F in $\psi'_{\text{AREA}_\theta}$

$$\psi\ \text{AREA} = \text{Dynamic stability} = \frac{1}{\psi'\text{AREA}} = \frac{1}{\text{cm.}}$$

Diagrams of Dynamic Stability

On the following pages diagrams are presented illustrating the methods of calculating dynamic stability.

EXPLANATION OF PLATE XIII

Definition of Dynamic Unstability.

Fig. 1. Physical significance of L_H, L_P, and L_L, on single frame of movie of disk descent.

Fig. 2.
Fig. 3.
Fig. 4.
Three possible situations in calculation of dynamic unstability, ψ $AREA_{\theta}$.

PLATE XIII

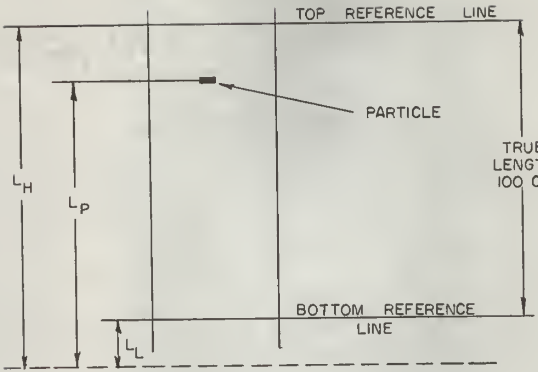

Fig 1

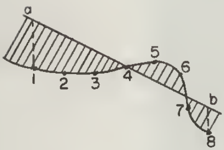

Fig. 2

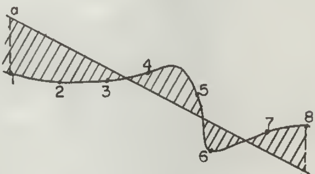

Fig. 3

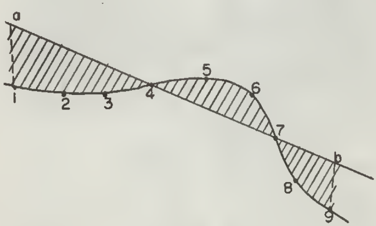

Fig. 4

EXPLANATION OF PLATE XIV

Definition of Dynamic Unstability, ψ'_{AREA_θ}

Fig. 1. Illustration of ψ'_{AREA_θ}, where shaded area adjacent to least squares line represents ψ'_{AREA_θ}.

Fig. 2.
Fig. 3. Illustration of application of trapezoid rule to calculating area, ψ'_{AREA_θ}.

Fig. 4. Illustration of calculation of area, ψ'_{AREA_θ}, in special case where trapezoid rule is not applicable.

PLATE XIV

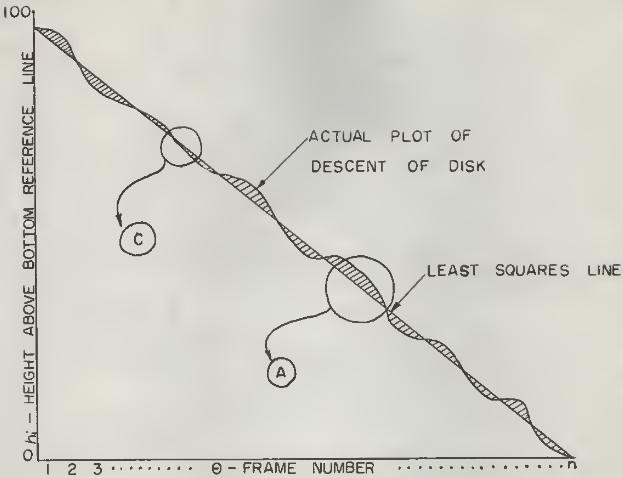

Fig. 1

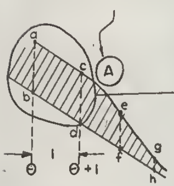

Fig. 2

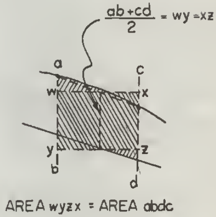

Fig. 3

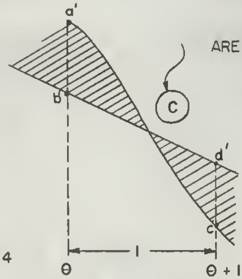

Fig. 4

GENERAL VISUAL OBSERVATIONS ON THE DESCENT OF DISKS THROUGH TRIETHYLENE GLYCOL AND WATER

Discussion of Observations and Postulations

Repeated observations were made of the general behavior of the disks as each descended through two separate fluid media; triethylene glycol and water. For water seventeen disks were investigated, while for triethylene glycol sixteen were investigated due to the buoyancy of disk one in the glycol. Preliminary to these investigations both faces of each disk were marked with a heavy black line corresponding to the diameter of the disk. In dropping these disks through either triethylene glycol or water the lines were visible to an observer looking down through the liquid column from a position above the drop tank. From this position any movement of the diameter of the disk in a plane parallel to the surface of the earth could be observed.

The disks were dropped in the fluid media at temperatures of $80^{\circ} \pm 3^{\circ}F$ for water and $90^{\circ} \pm 3^{\circ}F$ for triethylene glycol. At $80^{\circ}F$ the density of water was 0.9963 and at $90^{\circ}F$ that of one hundred per cent triethylene glycol was 1.115. However, at $90^{\circ}F$ the viscosity of triethylene glycol was 22 centipoises while at $80^{\circ}F$ that of water was approximately 0.037 times this or 0.82 centipoises.

Observations of the descents of each disk in triethylene glycol showed that the marked diameter normally did not rotate throughout the descent. With five observations of each disk this was observed in 96 per cent of all the observations. Of the disks in triethylene glycol which exhibited rotation of the marked diameter, this rotation appeared in only one out of five observations made on each of these disks. In all cases this rotation was observed to be less than 15°. In triethylene glycol the disk occasionally exhibited rotational motion of the diametrical axis of maximum slope, but even in the majority of these cases the marked diameter remained aligned with the direction which it assumed when released (See Fig. 2, PLATE XVII). These observations were tabulated in Table 10, Appendix.

In water, the less viscous media, the marked diameter showed decided deviations from the direction it assumed when initially released for 65 per cent of the one hundred observations. In water at 80° ± 3°F two of the heavier disks, 30 and 32, exhibited no diameter rotation over five observations of their descents. The remaining fifteen disks exhibited rotation of the marked diameter in from one to all of the observed drops. In the case of disks 19, 23, 40, 43, and 45, rotations first in one direction and then back in the other were noted in part of the observations. Also it was observed, by the utilization of a second observer watching perpendicular to the descent of the disk, that many of the rotations occurred after the disk had descended three-fourths of the depth of the column. These observations were tabulated in Table 11, Appendix.

Other observations were made on the path of motion which the center of the disk followed as it descended. When viewed from above the liquid column these observations showed that in ninety-seven per cent of five descents each of sixteen different disks the path of a given disk remained within one vertical plane. A sighting mechanism, built of welding bars, was constructed in the shape of a circle, the same size as the top of the drop column, and with a single bar as a diameter of the circle. The apparatus was fitted on the top of the drop column euch that as a disk descended it was possible to rotate the mechanism so that the diametrical bar was contained in the vertical plane through the path of motion of the descending disk. A pointer was added to the mechanism such that it pointed to values of angle inscribed along the rim of the drop column. The angle or angles between the vertical plane containing the disk path of motion and a vertical reference plane passing through 0° on the rim of the column were determined for four separate drops in triethylene glycol. These observations in Table 12, Appendix, showed that only 2 descents out of 64 exhibited a shift in the vertical plane passing through the path of motion of the disk through its 100 cm. descent.

No such conclusive observations were made for the seventeen disks descending in water. In water 57 per cent of the descents showed no single planar restriction of the path of motion as observed from the top of the column. Of the 43 per cent of the descents showing single planar motion 73 per cent of these observations were made on disks 20, 23, 27, 30, 32, 35, 37, and 40. In 32 per cent of the single planar motions the disk hit the side of the tank before the full 100 cm. between reference lines had been traveled. In no case did any disk show single planar wave, flutter, or oscillatory motion for all five observations in water at $80^{\circ} \pm 3^{\circ}$F. These observations were tabulated in Table 14, Appendix.

The observations in this study were restricted to disks descending in triethylene glycol and in water at Reynolds numbers above 78. After a multitude of observations, including those presented in Tables 13 and 14 of the Appendix, it was postulated that the disks descended in one or more of four main types of motion. These motions were named stable, flutter, wave, and spiral.

In stable motion the center of the disk fell along a vertical line. The vertical line was always perpendicular to the face of the disk. In triethylene glycol particles 6 and 46 descended in a stable manner in five out of five descents of each disk. In water no disk exhibited stable descent in any of the five drops tabulated in Table 14, Appendix. At least ten other drops not tabulated substantiated these observations over the same range of disks.

In flutter the disk exhibited what appeared to be a wobble or "teeter-totter" motion about a given fulcrum. This fulcrum consisted of one particular diameter of the disk; this diameter did not change on the disk throughout the descent. Flutter occurred while the center of the disk was descending through either a vertical line or a three dimensional curvelinear path. In triethylene glycol this diametrical fulcrum remained constant in direction throughout the descent.

In triethylene glycol disks 9, 13, 20, and 45 exhibited what was observed as flutter in one, two, or three descents out of five. Disks 19, 20, and 30 exhibited flutter as a component of wave motion. In water disks 13, 16, 19 and 20 appeared to descend with a flutter in at least one observation out of seven. In Table 14, Appendix, only five of these observations were tabulated. It was found in the case of flutter that a second or third observer sometimes viewed the motion as a small wave, instead of flutter. Thie led to later decisione concerning flutter as a postulated type of motion.

Wave motion was described as an oscillation of the center of the disk with the face of the disk always remaining perpendicular to the direction of motion (See Fig. 3, PLATE XV). In oscillation the path of motion of the center of the particle, when projected onto a vertical plane, appeared similar to a sine or cosine curve. As already described for descents in triethylene glycol a single vertical plane contained the entire path of oscillatory motion. For water this restriction to a single vertical plane did not apply, as oscillation and other motions in water were unmistakably three dimensional. In triethylene glycol 75 per cent of the 80 observations in Table 13, Appendix, revealed wave motion alone or in combination with flutter or disk rotation without diameter rotation. In water wave motion alone, or in combination with spiral or disk rotation with diameter rotation, appeared in 67 per cent of the 85 observations of 3 drops in Table 14, Appendix. Spiral was defined as a "cork screw" path of motion of the center of the disk (See Fig. 1, PLATE XVII). In Table 13, Appendix, spiral motion did not appear in 5 drops through triethylene glycol. Other observations made in this study, but not tabulated, substantiated this. In water disk one exhibited exclusively spiral motion over three drops as shown in Table 14, Appendix. In 29 per oent of the total observations of seventeen disks in Table 14, Appendix, spiral motion appeared either alone or as an extension of wave motion and flutter. The two dimensional appearances of these motions were illustrated in PLATES XV and XVII.

Other postulated types of motion were also recognized but these motions only seldom or never appeared in triethylene glycol. The nomenclature given two of these motions were disk rotation without diameter rotation and disk rotation with diameter rotation. In both cases disk rotation was basically defined as rotation of the diametrical axis of maximum slope of a disk. In the former case the disk did not actually rotate, but, without a diameter reference mark, appeared to do so (See Fig. 2, PLATE XVII). In the latter case the disk rotated as apparent from the rotation of a marked diameter on the face of the disk (See Fig. 3, PLATE XVII). It was found that some discernment was necessary in distinguishing between borderline cases of spiral, disk rotation, and wave.

If the motion, appearing as a wave over a small increment of the total descent, exhibited at the same time one complete loop of a spiral over the total descent it was then classified as spiral instead of wave. If the motion appearing as a disk rotation exhibited any recognizable segment of a spiral loop over the total descent, it was classified as a spiral. In the case of disk rotation and wave motion together, the combination was treated as wave motion with rotation. Infrequently, in only 5 per cent of the observations in Table 13, Appendix, disk rotation without diameter rotation appeared in triethylene glycol, while disk rotation with diameter rotation did not appear in any of the 80 observations. In water, disk rotation with diameter rotation appeared in less than 5 per cent of the observations in Table 14, Appendix, while disk rotation without diameter rotation was not apparent in any of the 85 observations. Diameter rotation in water was most closely associated with spiral motion as was seen from a comparison of Tables 11 and 14, Appendix. These were illustrated in PLATE XVII.

At this point it was discovered that fairly accurate reproductions of the disk path of descent could be obtained. This was accomplished by tracing with a pencil the projected image of the disk from each movie frame, as each frame in turn, was projected onto a screen of white paper. Prior to tracing, each frame was adjusted to the position on the screen which corresponded to that previously occupied by the preceding frame traced. This positioning was accomplished by adjusting the upper reference line pictured on each frame of the movie to a constant reference point on the white paper background; by this technique a fairly accurate reproduction of the overall path of descent was obtained. Only parts of the six descents filmed were analyzed in this manner due to the excess time and personnel requirements.

From these sketches more exacting pictures of the postulated types of motions of disks in triethylene glycol were established. The results of analysis of these sketches were tabulated in Table 15, Appendix. It was found that flutter was merely wave motion with barely perceptible horizontal displacement when viewed at the true velocity of descent. This observation was further substantiated by analyzing the remainder of the movies. For this analysis a vertical reference line was established by holding a white string vertically downward from the initial projected position of a disk as viewed on the movie screen. The projection of the disk was carefully observed as it descended along the string on the screen. Horizontal displacements to the right and left of this line immediately showed up on all the disks which had been formerly depicted as descending with a fluttering motion. These same operations, also, showed that the disks depicted as settling in stable motion did indeed settle in that manner. Typical results of these latter analyses were also tabulated in Table 15, Appendix.

From these newer approaches to observing motion it was postulated that wave motion actually consisted of three types. That previously classified as wave motion was reclassified as two types of motion - wave I and wave III. Wave I was subtyped as wave I-A and wave I-B.

Wave, as previously defined, became wave I-A. It was noted that wave I-A consisted of planar oscillatory motion and it was postulated that the disk always maintained orientation such as to offer the face of greatest resistance perpendicular to the path of motion of the center of the disk. Wave I-B motion was observed as similar in definition to wave I-A motion, but without the restriction that the face of greatest resistance always be perpendicular to the path of the center of the disk. Analysis of sketches of disk descents showed that as a disk became heavier its increased moment of inertia prevented it from behaving as a wave I-A disk. It was impossible to discern between these two types of motion on the sketches of the disk descent. However, as the moment of inerita of the disks increased, wave I-A and wave I-B motions formed a logical sequence between stable and wave III motions. Wave I-B motion was definitely observed in disks 19, 20, 23, and 27. However, for disks 9, 13, and 16 there was little to discern between the types of motion, since the sketches were not refined enough to allow precision study. The heavier a disk became the larger the absolute difference of $\theta - 90^{\circ}$ became. θ represented, at any instant, the smallest angle between the plane of the leading face of the disk and the directional vector of the center of the disk. Disks exhibiting wave I-A and I-B motion, at least once, were 16, 19, 20, 23, 27, and 30. These motions are illustrated in PLATES XV, XVI, and XVII.

When the plane containing the face of a disk rotated away from the horizontal through the vertical and back to the horizontal wave III motion was observed. It was postulated that the angle between the plane containing the face of the disk and a horizontal plane became increasingly larger as the disk descended until the disk turned over or flipped. Flip was defined as the motion of a disk where the lower face of the disk interchanged with the upper face through a 180° rotation. Disks exhibiting wave III motion were disks with large moments of inertia with respect to their weights. In all cases they were of steel rim and plastic core construction. Therefore this flipping action was a result of the large moments of inertia of these disks. This was a reasonable conclusion when it was considered that a baton is constructed of a shaft with heavy weights at each end such that it has a large moment of inertia.

The motions described here and illustrated in PLATE XVI can be observed by the use of a sheet of typing paper. A rectangle 4 by 1½ inches cut from the sheet and dropped face down from shoulder high exhibits wave III motion. A square consisting of three 2½ by 2½ pieces glued together exhibits either wave I-A or wave I-B motions.

Further observations concerned the frequencies of planar oscillation of disks descending in wave patterns. From the sketches prepared for Table 15, Appendix, the following frequencies in cycles per 100 cm. descent were observed for parts of two different drops.

Table 1: Frequencies in Cycles per 100 cm. Descents of Disks.

Disk Number	Drop One	Drop Two
9	—	6
13	—	6
16	6	6
19	6	5½
20	—	5 3/5
23	5	—
27	4 3/4	—
30	4	—
32	4	—
35	—	—
37	3 2/3	—
40	—	—

Diagrams of Postulated Types of Motion

On the following pages diagrams are presented illustrating the postulated types of motion of disks descending in triethylene glycol and water.

EXPLANATION OF PLATE XV

Postulated types of motion of disks descending in a fluid media.

Fig. 1. Stable descent.

Fig. 2. Flutter.

Fig. 3. Wave I-A, one of two possible subtypes of Wave I.

PLATE XV

STABLE DESCENT

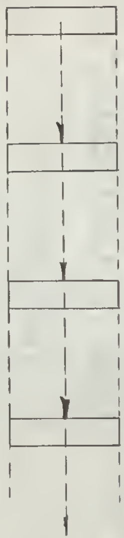

Fig. 1

FLUTTER

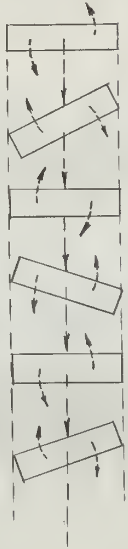

Fig. 2

WAVE I-A

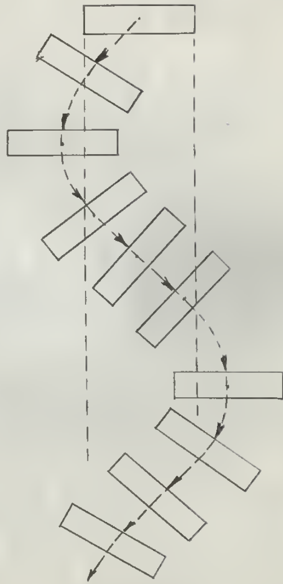

Fig. 3

EXPLANATION OF PLATE XVI

Postulated types of motion of disks descending in a fluid media.

Fig. 1. Wave I-B, the other subtypes of Wave I motion.

Fig. 2. Wave III.

PLATE XVI

WAVE I-B

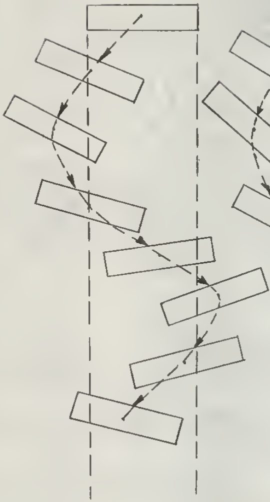

Fig. 1

WAVE III

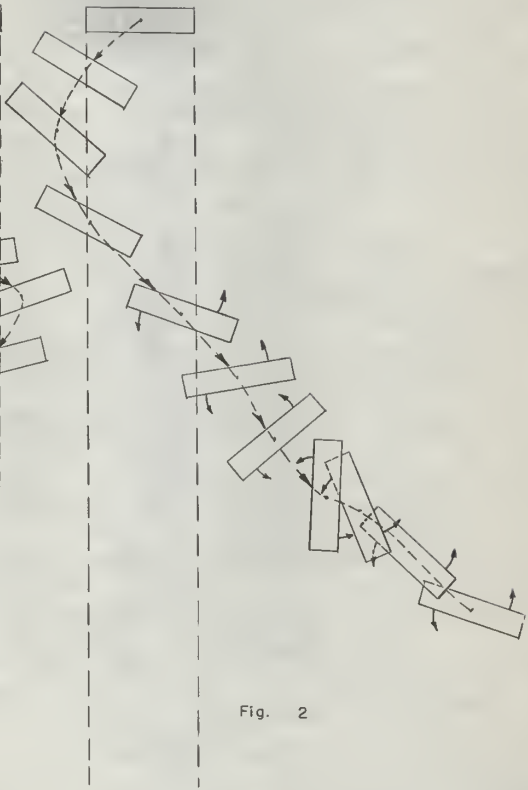

Fig. 2

EXPLANATION OF PLATE XVII

Postulated types of motion of disks descending in fluid media.

Fig. 1. Spiral.

Fig. 2. Disk rotation without diameter rotation.

Fig. 3. Disk rotation with diameter rotation.

PLATE XVII

SPIRAL

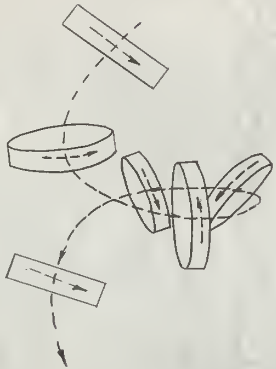

Fig. 1

DISK ROTATION
W/O DIAMETER ROTATION

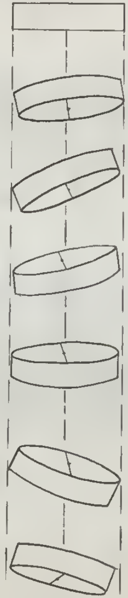

Fig. 2

DISK ROTATION
WITH DIAMETER ROTATION

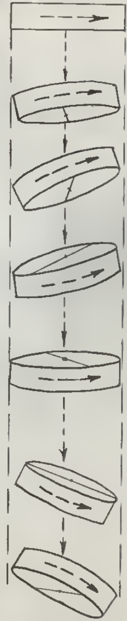

Fig. 3

EXPLANATION OF PLATE XVIII

Illustrations of ascent of air bubble and descent of flat solid.

Fig. 1. Ascent of air bubble.

This illustration was acquired from Fig. 12 of Reference 5.

Fig. 2. The track of a flat solid.

This illustration was acquired from Reference 9.

PLATE XVIII

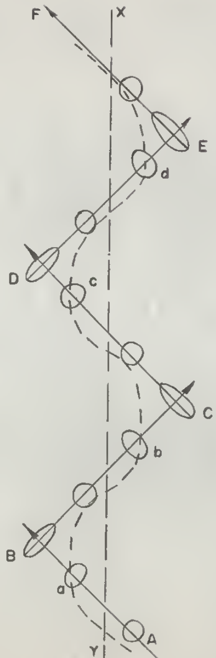

Fig I

Fig. 2

EVALUATION OF DATA AND PRESENTATION OF RESULTS

Dynamic stabilities were calculated by three methods; each method was previously described. The dynamic stabilities evaluated were $\psi s^2_{y.x}$, reciprocal of mean square deviation from regression, $\psi\sqrt{s^2_{y.x}}$, reciprocal of sample standard deviation from regression, and ψ_{AREA}, reciprocal of mean area between least squares line and path of disk descent. These values for three drops were tabulated in Tables 7, 8, and 9 of the Appendix. Obvious differences existed between the dynamic stabilities calculated by any one method for each disk over its three descents. The more outstanding reasons for these differences were the randomness of free-fall descents of disks in fluids, the paralactic errors, the measuring errors, and the extraneous disturbances, as described in the procedure, in the fluid media during descents of the disks.

It was impossible to distinguish between true randomness of motion and erraticness of motion which was induced by extraneous disturbances. Extraneously induced disturbances in the fluid were assumed to be sufficiently dampened by the precautions earlier described in the procedure, although these steps certainly guaranteed no possibility for complete removal of this source of error. Measuring errors, a result of obtaining values of disk height from motion pictures of disk descents, provided measureable but unpredictable sources of disagreement, dictated by equipment, personal, and environmental deficiencies at any time. Parallax - as treated by Himes (3) - also afforded measureable sources of error, where the magnitude of paralactic error was determined, for the

EXPLANATION OF PLATE XIX

Illustration of 90% confidence intervals on $\psi\sqrt{s^2_{y.x}}$, dynamic stability, for range of disks investigated.

upper and lower limits of 90% confidence intervals.

X Drop 1.

O Drop 2.

□ Drop 3.

PLATE XIX

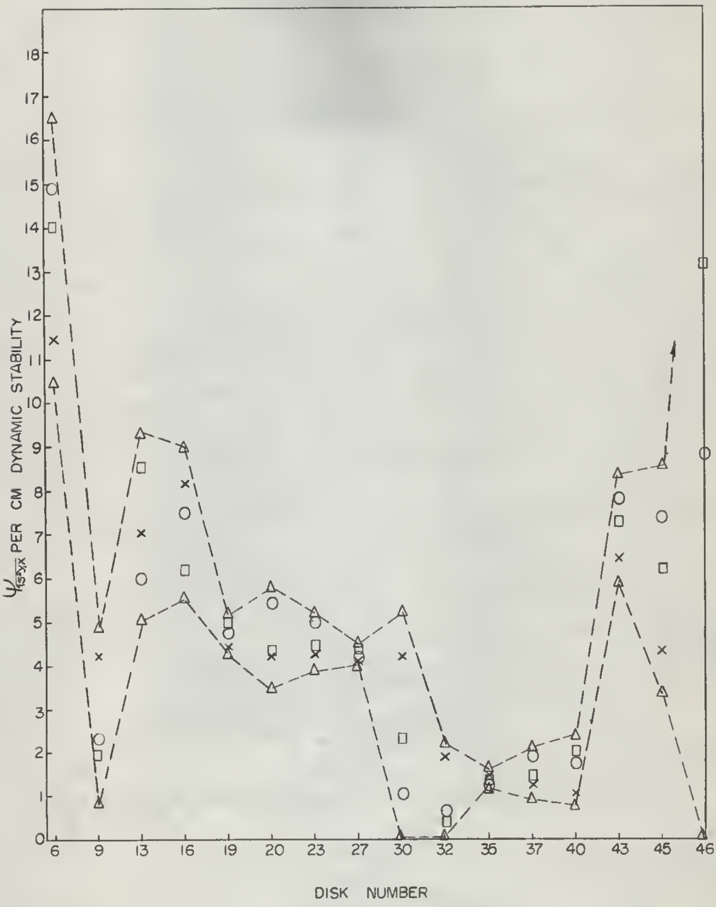
$\psi_{\overline{(s^2_{y,x})}}$ PER CM DYNAMIC STABILITY
0
1
2
3
4
5
6
7
8
9
10
11
12
13
14
15
16
17
18
6 9 13 16 19 20 23 27 30 32 35 37 40 43 45 46
DISK NUMBER

EXPLANATION OF PLATE XX

Plots of $\psi\sqrt{s^2_{y.x}}$, dynamic stability, for three drops over entire range of disks showing intensities of $\psi\sqrt{s^2_{y.x}}$ in relation to postulated types of motion.

X Drop 1.

O Drop 2.

□ Drop 3.

upper and lower boundaries on ranges of $\psi\sqrt{s^2_{y.x}}$.

PLATE XX

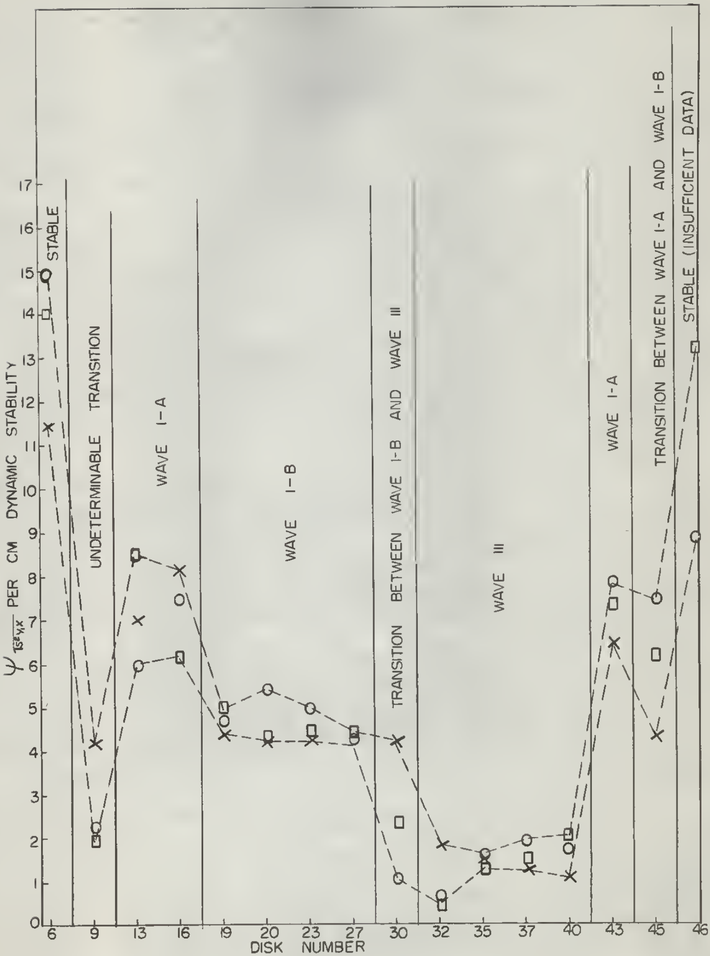
$\psi_{15^\circ y,x}$ PER CM DYNAMIC STABILITY
DISK NUMBER
6 9 13 16 19 20 23 27 30 32 35 37 40 43 45 46
0 1 2 3 4 5 6 7 8 9 10 11 12 13 14 15 16 17
STABLE
UNDETERMINABLE TRANSITION
WAVE I-A
WAVE I-B
TRANSITION BETWEEN WAVE I-B AND WAVE III
WAVE III
WAVE I-A
TRANSITION BETWEEN WAVE I-A AND WAVE I-B
STABLE (INSUFFICIENT DATA)

EXPLANATION OF PLATE XXI

Plots of ψ_{AREA}, dynamic stability, for three drops over entire range of disks.

X Drop 1.

O Drop 2.

□ Drop 3.

upper and lower boundaries on ranges of ψ_{AREA}.

PLATE XXI

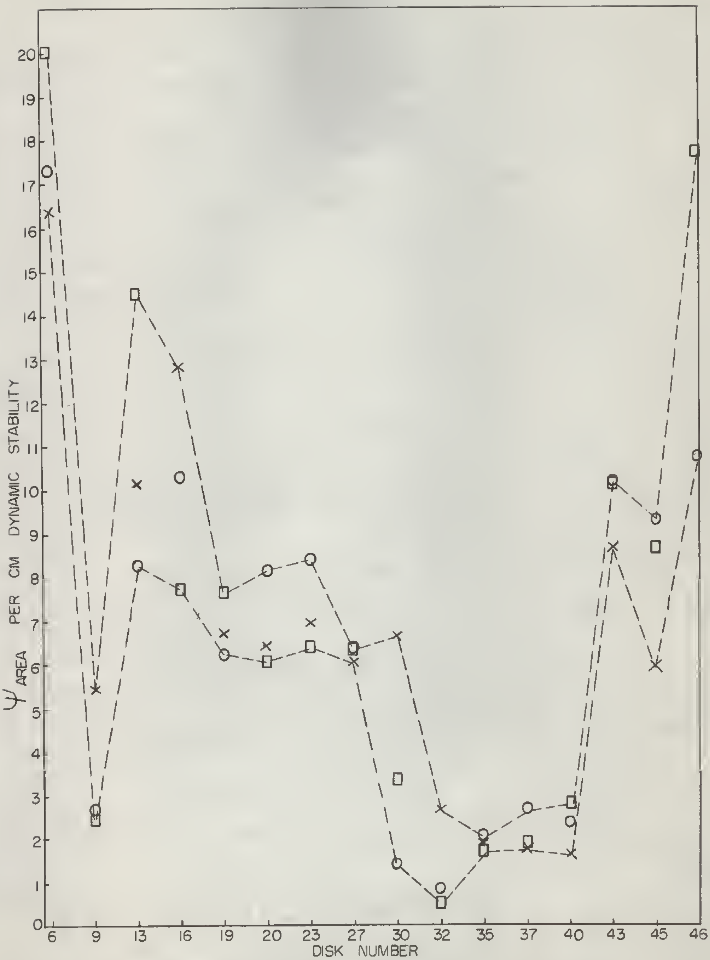

ψ_{AREA} PER CM DYNAMIC STABILITY
DISK NUMBER
0
1
2
3
4
5
6
7
8
9
10
11
12
13
14
15
16
17
18
19
20
6
9
13
16
19
20
23
27
30
32
35
37
40
43
45
46

EXPLANATION OF PLATE XXII

Plots of $\psi s^2_{y.x}$, dynamic stabilities for three drops over entire range of disks.

X Drop 1.

O Drop 2.

□ Drop 3.

upper and lower boundaries on range of $\psi s^2_{y.x}$.

PLATE XXII

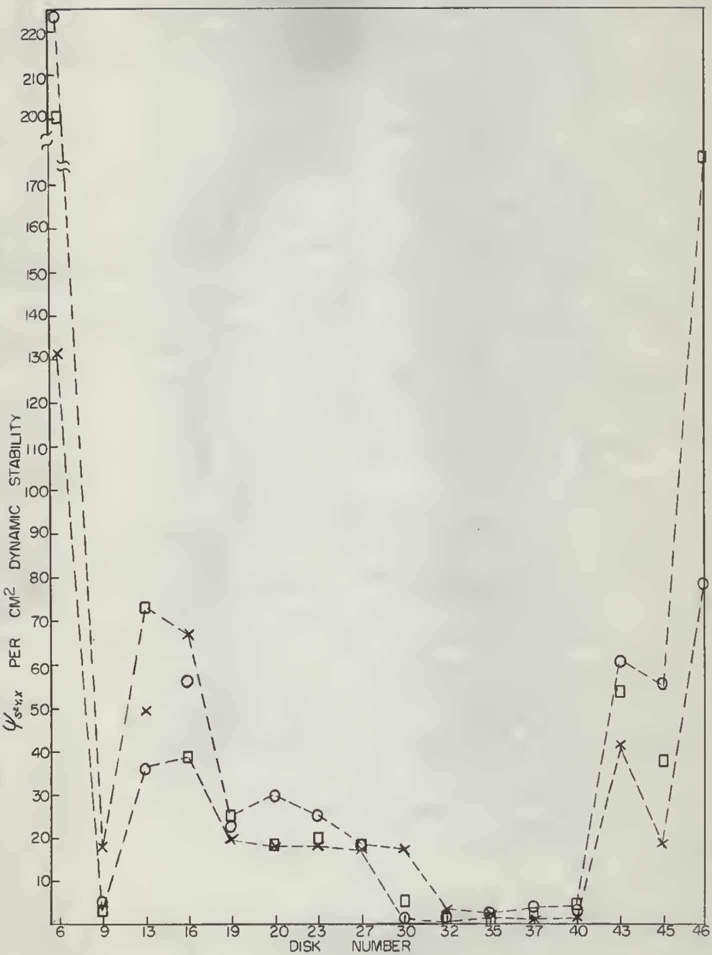
220
210
200
170
160
150
140
130
120
110
100
90
80
70
60
50
40
30
20
10
$\psi_{s^2y.x}$ PER CM^2 DYNAMIC STABILITY
6
9
13
16
19
20
23
27
30
32
35
37
40
43
45
46
DISK NUMBER

EXPLANATION OF PLATE XXIII

Bar graph illustrating relationship of 90% confidence intervals of $\psi\sqrt{s^2_{y.x}}$, dynamic stabilities, of disks classified according to postulated types of motion.

PLATE XXIII

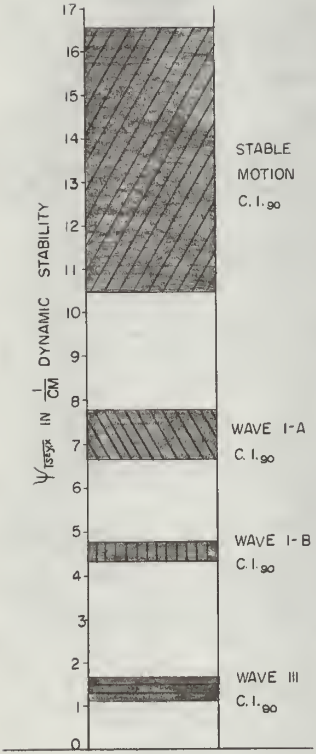

17
16
15
14
13
12
11
10
9
8
7
6
5
4
3
2
1
0
$\psi_{\sqrt{s^2_{yx}}}$ IN $\frac{1}{CM}$ DYNAMIC STABILITY
STABLE MOTION
C. I.$_{90}$
WAVE I-A
C. I.$_{90}$
WAVE I-B
C. I.$_{90}$
WAVE III
C. I.$_{90}$

EXPLANATION OF PLATE XXIV

Graph of properties of disks for three drops in relation to postulated types of motion assigned each disk.

○ weight of disk.

□ density of disk.

× core diameter of disk.

△ moment of inertia of disk.

PLATE XXIV

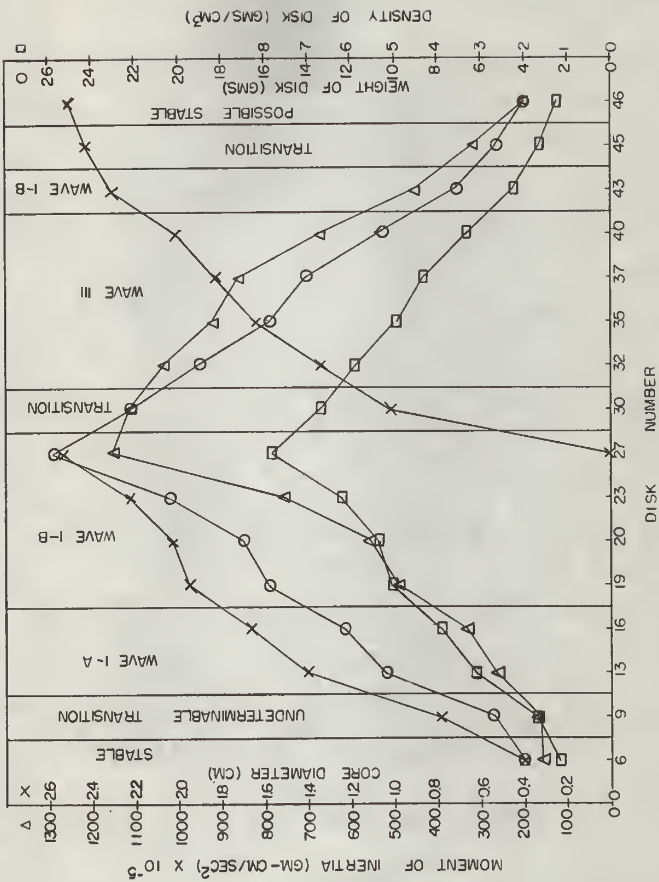
MOMENT OF INERTIA (GM-CM/SEC²) X 10⁻⁵
CORE DIAMETER (CM)
WEIGHT OF DISK (GMS)
DENSITY OF DISK (GMS/CM³)
DISK NUMBER
STABLE
UNDETERMINABLE TRANSITION
WAVE I-A
WAVE I-B
TRANSITION
WAVE III
WAVE I-B
TRANSITION
POSSIBLE STABLE

EXPLANATION OF PLATE XXV

Graph of Reynolds Numbers of disks for three drops in relation to postulated types of motion assigned each disk.

$Re = \frac{D_s v \rho}{\mu}$, where

$D_s =$ diameter of sphere having same volume as disk in ft.

$v =$ velocity of disk in ft./sec.

$\rho =$ density of fluid in lb./ $ft.^3$

$\mu =$ viscosity of fluid in Bvu, lb./ft. sec.

$\times$ Drop 1.

$\square$ Drop 2.

Δ Drop 3.

PLATE XXV

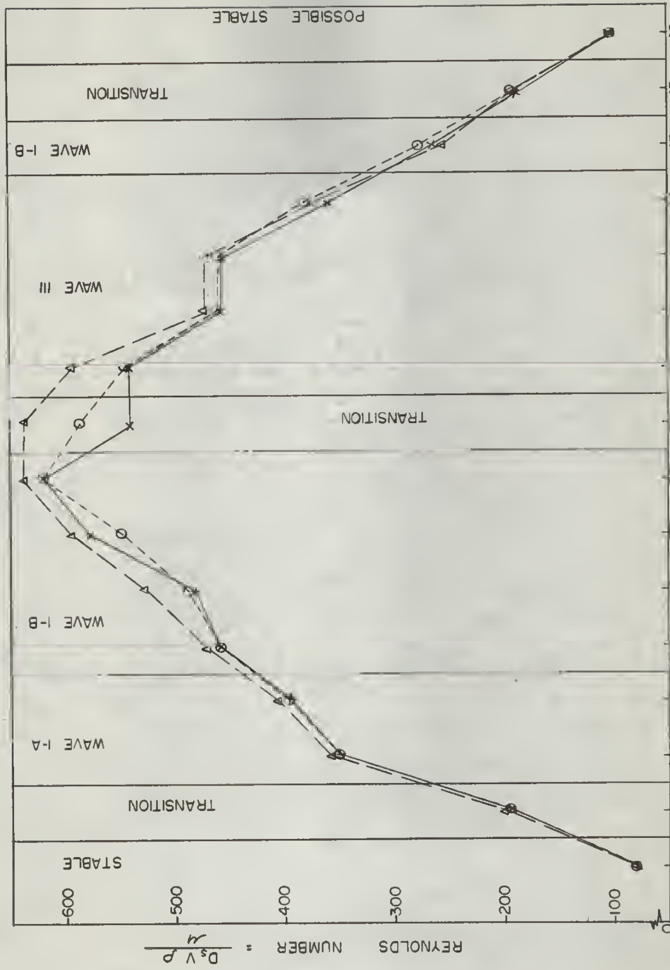
STABLE
TRANSITION
WAVE I-A
WAVE I-B
TRANSITION
WAVE III
WAVE I-B
TRANSITION
POSSIBLE STABLE
6
9
13
16
19
20
23
27
30
32
35
37
40
43
45
46
DISK NUMBER
0
100
200
300
400
500
600
REYNOLDS NUMBER = $\frac{D_s V \rho}{\mu}$

major part, by the position of the particle relative to the location of the reference wires and to the location of the camera. By moving the camera to a position further from the drop column the parallax was lessened by a calculable amount. However, the allowable distance between the camera and the tank was limited by the characteristics of the available telescopic lenses.

In summary extraneously induced disturbances of the descent of a disk and randomness of behavior in the descent of a disk provided incalculable and uncontrollable sources of disagreement between measured paths of descents. Measuring error was calculable but uncontrollable, while parallax was both calculable and controllable within equipment and camera limitations. Therefore, it remained to minimize paralactic error to the degree where it was of the same or of a lesser magnitude than measuring error. Without altering the original locations of the reference wires this was accomplished by increasing the distance between the camsra and the drop column to the maximum allowed by the available telescopic lenses. Confidence intervals on maximum measuring error when compared with maximum possible paralactic error were found to be of the same range of magnitude. This comparison was presented in PARALLAX (3) in conjunction with a rigorous investigation of parallax.

Other sources of error were due to the non-uniformity of release of the disks and sizs limitations of the drop column. The former was minimized by disregarding an initial length of each descent while the latter was unavoidable for monstary reasons. Another source of error resulted from variations in the rate at which the camera filmed the descent. The spesd of the camera was found to vary from 16.5 to 19.6

frames per second. This meant that the relative magnitude of each frame varied within a given descent. The assumption that all frames were equal to the same increment of time was not true. This variation was a characteristic of the spring and governor regulating the camera speed. It, also, depended upon how often and to what degree the photographer wound the camera. For this reason it was impossible to calculate the magnitude of this source of error. The solution to this problem lay in the statement, "An ounce of prevention is worth a pound of cure". However, "the ounce of prevention," consisted of a synchronizing motor attachment for the camera. Monetary limitations prevented this. However, after some consideration it was felt that this lack of uniformity in the camera speed was not nearly as critical as measuring and paralactic errors, since the variation of camera speed within any one descent was extremely small. This was borne out by the excellent agreement between the calculated dynamic stabilities of various descents of most disks.

The values of dynamic stability by each method - $\psi\sqrt{s^2_{y.x}}$, ψ_{AREA}, $\psi\, s^2_{y.x}$, - were plotted in PLATES XX, XXI, and XXII, respectively. The method based upon $\psi\sqrt{s^2_{y.x}}$ was randomly chosen from these three for further consideration. In PLATE XIX, $\psi\sqrt{s^2_{y.x}}$ was plotted as the upper and lower limits of 90 per cent confidence intervals on the dynamic stabilities of each disk. This graph illustrated the statement that the true value of dynamic stability for each disk had a 90 per cent chance of lying between the individual limits described. This did not state that the true curve of dynamic stability had a 90 per cent chance of lying entirely between these limits formed by connecting the individual limits. However, the limits so acquired by connecting these individual limite lead to the statement that each point of the true curve of dynamic stabilities had a 90 per cent chance of lying within theee limits.

During the period of calculation of dynamic stabilities a completely isolated etudy was being conducted on the types of motion apparent in the disk deecents. As was described earlier in thie thesis under General Visual Observations on the Descent of Disks through Triethylene Glycol and Water each disk was assigned to one of three main types of motion. In PLATE XX the rangee of assigned motions were compared with the magnitudee of dynamic stabilities. In PLATE XXIV, a similar comparison was made between physical characteristics of the disks and assigned motions. In PLATE XXV, a like comparison was made between Reynolde numbers and aseigned motions.

DISCUSSION OF RESULTS

With reference to Tables 7, 8, and 9 of the Appendix, it is seen that decided agreements between dynamic stabilities of the three descents of each disk were clearly observed for most of the disks. Disks not exhibiting this agreement were numbers 9, 30, 32, and 45. In these cases the dieagreements, relative to the magnitudes of the dynamic stabilities, were large. Erratic behavior in the eource of a measurable quantity was aeeociated by this inveetigator with the inability to reproduce measuremente of that quantity. Therefore, becauee of the visually observed erraticalness of disks 30, 32, 35, 37, and 40 during their descente disagreement was expected, although only disks 30 and 32 actually exhibited any marked diversion. This indicated some degree of uniformity of behavior within the erraticalness. Erraticalnese in the descent of a disk wae also associated with low dynamic stabilities. This was true; diske 32, 35, 27, and 40 had the lowest valuee of dynamic stability.

Dynamic stabilities, $\psi\sqrt{s^2_{y.x}}$, ψ_{AREA}, and $\psi s^2_{y.x}$, were plotted on PLATES XX, XXI, and XXII, respectively. From the plots of all three methods four levele of magnitudes of dynamic stability were apparent. Selecting $\psi\sqrt{s^2_{y.x}}$ for further study, it was found that disk 6, the most stable, formed the highest level. Disks 13, 16, and 43 formed the second level. Diske 19, 20, 23, and 27 formed the third. Disks 32, 25, 27, and 40 formed the lowest and final level. Disks 9, 30, and 45 had values of dynamic stability in more than one level. With only two values of dynamic stability it was improper to classify diek 46 in any of the levels.

The four levels were then compared with the postulated types of motion exhibited by the descending disks, Table 15, Appendix. This study, dealing with the types of motion, was conducted prior to and separate from the evaluation of dynamic stabilities. Therefore, the excellent agreement of the two wae surprieing. These postulated types of motion were compared with dynamic stabilities on the plot of $\psi\sqrt{s^2_{y.x}}$ againet diek number, PLATE XX. The diecrepancies caused by dieks 9, 30, and 45 were resolved by considering these disks as transitional between two types of motion. Table 15, Appendix, substantiated this for disk 30, since this disk was found to exhibit more than one type of motion. Disk 43 was observed to exhibit wave I. Its values of dynamic etability did not, however, indicate to which eubtype it belonged. Since one value of dynamic stability on disk 43 fell into the wave I-A level and the other two into the wave I-B level, disk 43 was finally classified as transitional between wave I-A and wave I-B. Disk 9 presented the only outstanding discrepancy in that the observed motion, postulated as wave I, did not agree with the levels in which its dynamic stabilities fell - wave I-B and wave III. Therefore, disk 9 was claesified as being in an undeterminable transition region.

Ninety per cent confidence intervals were calculated on the three values of dynamic stability for each disk, as preeented in Table 3, Appendix. The cloee agreement between the confidence intervals on dynamic etability among various disks within a given type of fall indicated that the dynamic stabilities for these disks came from the same populations. The disks having comparable confidence intervals were found to form four separate groups. These four groups corresponded exactly to the four levele of dynamic etability earlier found to correspond to the postulated types of motion. Therefore, the values of dynamic stability for each disk, with the exceptions of 9, 30, and 45, fell into one of the postulated types of motion. Ninety per cent confidence intervals were then calculated on each group as presented in Table 4, Appendix. The limits on these groups, or levels, were then presented ae a bar graph in PLATE XXIII. This illustrated the etatement that the true value of dynamic stability for each of these groupe had a 90 per cent chance of lying within the limits, indicating that each such level was distinct and separate from the others.

The next step was to make an attempt to correlate the properties of the disks and fluid to the aseigned typee of motion. The properties of the disks were tabulated in Table 5, Appendix, and plotted in conjuction with the types of motion assigned each disk in PLATE XXIV. From Tables 7, 8, and 9 of the Appendix Re's were plotted in the same manner in PLATE XXV. From PLATE XXIV the only conclusive statement possible was that disks exhibited greater unstability as their moments of inertia became large relative to their weights. Stable motion occurred at low weights, low moments of inertia, and low densities relative to the comparable properties for disks which exhibited other postulated types of motion. Disk 6 exhibited stable motion. Finally, from PLATE XXV, the Reynolds numbers, based on D_s, for the three descents of disk 6 were less than 100. Disks exhibiting waves I-A, I-B, and III motion had Re's of 275 to 325, 225 to 650, and 300 to 625, respectively.

CONCLUSIONS

The most significant conclusion, based upon more than 41,000 measurements, was that dynamic stability of disks is measureable and therefore exists.

It was concluded that a disk, in a free-fall descent, exhibited one of three postulated types of motion; i. e. stable, wave I, or wave III. It was further postulated that wave I motion consisted of subtypes; wave I-A and wave I-B. The distinction between these subtypes appeared in the measured dynamic stabilities; corresponding to the exact boundary predicted by the observations (See Table 15, Appendix). In water disks exhibited three main types of motion; i. e. wave, spiral, or disk rotation with diameter rotation, or combinations of these. For triethylene glycol a definite relationship was found between these motions and dynamic stability, $\psi\sqrt{s^2_{y.x}}$.

Table 2: Relationship Between Types of Motion and $\psi\sqrt{s^2_{y.x}}$.

Disk number	Postulated type of motion	Range of dynamic stabilities, 1/cm.
6	Stable	11.49 to 14.92
13, 16, and 43	Wave I-A	6.02 to 8.55
19, 20, 23, and 27	Wave I-B	4.15 to 5.46
32, 35, 37 and 40	Wave III	0.44 to 2.01

Each range of dynamic stabilities corresponding to a particular type or subtype of motion was distinct and separate from any of the others. By applying confidence intervals to these ranges it was shown that the true value of dynamic stability for each type of motion had a 90 per cent chance of lying within limits which did not overlap the limits of other types of motion.

Actually, three methods, $\psi\sqrt{s^2_{y.x}}$, $\psi\ s^2_{y.x}$, and ψ_{AREA} were used in calculating dynamic stability. The method based upon $\psi\sqrt{s^2_{y.x}}$ was randomly chosen from these three for further consideration.

From a comparison of physical properties of the disks against the types of motion into which each disk fell it was found that a low dynamic stability was associated with a high moment of inertia relative to the weight of the disk. This is summarized in PLATE XXIV.

From a comparison of Reynolds numbers for each disk with the types of motion of each disk it was concluded that a Re, based on D_s, of one hundred or less was associated with stable motion. Disk 6, the only disk which clearly exhibited stable motion, was the lightest one and it also had the least density and moment of inertia of all those investigated.

These conclusions were all restricted to disks which descended in triethylene glycol at 88 to 90°F at Re, based on D_s, ranging from 78 to 640.

RECOMMENDATIONS

The following are recommended for immediate investigation:

1. Paralactic error may be noticeably reduced by moving the reference wires to a position in contact with the drop column. This suggests an investigation of the positioning of the top reference wire immediately above the release mechanism and the bottom reference wire inside the column near the bottom.

2. Parallax may be further reduced by removing the camera further from the drop column, thus suggesting that an investigation be made of telescopic lenses allowing this increased distance.

3. Recent films of disk descents revealed that a suspension of rust pigments in the triethylene glycol produced more distinct pictures of the disks. Other pigments may prove even more satisfactory.

4. Error, although not significant when compared to paralactic and measuring errors, was introduced into the final values of dynamic stability due to the non-uniformity of the camera speed. It is possible to rectify this by the use of a synchronizing motor. As paralactic and measuring errors are decreased this consideration will become important.

5. Measuring errors and measuring time could be noticeably decreased by moving the dark room and projector to a location supported by concrete flooring.

6. The size of the drop column should be appreciably increased. An increased diameter would lessen wall effects, while both an increased diameter and length would allow a more thorough study of disks exhibiting wave III motion.

The following are recommended for long-range investigation:

1. An analysis should be made of the possibility of using a radioactive source to expose film strips attached to the drop column to obtain a continuous picture of the disk descent.

2. A survey should be made of the possibility of employing either electric eyes or magnetic coils along the length of the column, such that with the addition of an appropriate recorder, readings of particle height may be directly obtained.

3. A study should be made of drop tanks other than cylindrical in shape.

Statements could be made concerning what next should be investigated, but dynamic stability has revealed such a fertile field as to make any recommendations for future work little more than twigs in an ocean, therefore, such concern will be left to the interests of future investigators.

ACKNOWLEDGMENTS

Some of the early experimental work which contributed to this thesis was conducted by Karl Mohn and Roger D. Allen, former students at Kansas State University, under the supervision of Assistant Professor Raymond C. Hall. The computer programs included in this thesis were prepared by Dr. Thomas S. Parker and Thomae L. Hamilton of the IBM 650, Kansas State University. Both Dr. Parker and Mr. Hamilton, afforded this author much of their valuable time in supervising the evaluation of dynamic stability in the IBM 650. The disks used in this etudy were percision conetructed by Mr. Andy Andereon of Building and Repair, Kaneas State University.

The most important contribution was certainly that of Profeseor Hall, whoee patience, pedagogical judgement, and interest removed untold pitfalls to the successful completion of this work.

Another extremely important contribution was that of the author's wife, Francee B. Himes, who provided a never ending source of inepiration, patience and understanding.

A most deserving acknowledgment is, also, given to Dr. Henry T. Ward, Professor and Head of the Chemical Engineering Department.

The funde making this work possible were provided by the Agricultural Experiment Station of Kansae State University.

REFERENCES

(1) Becker, H. A.
The effects of shape and Reynolds number on drag in the motion of a freely oriented body in an infinite fluid. The Canadian Journal of Chem. Engg., 85. April, 1959.

(2) Dow Glycols, The Dow Chemical Company. Midland, Michigan. 1947.

(3) Himes, B. L., Sr.
Parallax and moments of inertia of disks employed in study. Unpublished report, Dept. of Chemical Engineering, Kansas State University, 1959.

(4) Mickley, H. S., T. K. Sherwood, and C. E. Reed. Applied Mathematics in Chemical Engineering. New York: McGraw - Hill Book Company, Inc., 1957.

(5) Miyagi, Otogoro
Motion of an air bubble rising in water. Philosophical Magazine and Journal of Science. London. L: 125. 1925.

(6) Pettyjohn, E. S. and E. B. Christiansen
Effect of particle shape on free-settling rates of isometric particles. Chem. Engg. Progress. 44: 169. 1948.

(7) Squires, Lombard and Walter Squires Jr.
The sedimentation of thin disks. Transitions of the American Inst. of Chem. Engg. 33: 3. 1937.

(8) Wadell, H.
The coefficient of resistance as a function of Re. for solids of various shapes. Journal of the Franklin Institute. 217: 459. 1930.

(9) Wetherall, E. W.
The track of a flat solid through water. Nature. 60: 845. 1922.

APPENDIX

Table 3. Calculation of C. I.$_{90}$ on Dynamic Stabilities

Disk Number	$\psi\sqrt{s^2_{y.x}}$ 1/cm Drop 1	Drop 2	Drop 3	X_1 Average	$\sum(X_{1_k} - X_1)^2$	$\sqrt{S^2_m}$	90% Confidence Intervals (4)
6	11.49	14.92	14.08	13.50	6.39	1.03	$10.49 \leq x_1 \leq 16.51$
9	4.26	2.34	1.99	2.86	2.90	0.70	$0.82 \leq x_1 \leq 4.90$
13	7.04	6.02	8.55	7.20	3.24	0.73	$5.07 \leq x_1 \leq 9.33$
16	8.20	7.52	6.21	7.31	2.04	0.59	$5.60 \leq x_1 \leq 9.02$
19	4.46	4.78	5.03	4.76	0.16	0.16	$4.29 \leq x_1 \leq 5.23$
20	4.26	5.46	4.29	4.67	0.93	0.40	$3.52 \leq x_1 \leq 5.82$
23	4.29	5.02	4.44	4.58	0.30	0.22	$3.93 \leq x_1 \leq 5.23$
27	4.15	4.24	4.44	4.28	0.04	0.08	$4.03 \leq x_1 \leq 4.53$
30	4.22	1.09	2.35	2.55	4.96	0.91	$0.00 \leq x_1 \leq 5.21$
32	1.86	0.68	0.44	0.99	1.16	0.44	$0.00 \leq x_1 \leq 2.27$
35	1.48	1.56	1.29	1.44	0.04	0.08	$1.21 \leq x_1 \leq 1.67$
37	1.28	1.97	1.44	1.56	0.26	0.21	$0.95 \leq x_1 \leq 2.17$
40	1.09	1.74	2.01	1.61	0.45	0.27	$0.81 \leq x_1 \leq 2.41$
43	6.41	7.81	7.30	7.17	1.03	0.41	$5.96 \leq x_1 \leq 8.38$
45	4.35	7.41	6.17	5.98	4.73	0.89	$3.39 \leq x_1 \leq 8.57$
46*	----	8.85	13.16	11.00	9.28	2.15	$0.00 \leq x_1 \leq 24.57$

D. F. = 3 - 1 = 2 $t_{0.10} = \pm 2.920$

*D. F. = 2 - 1 = 1 $t_{0.10} = \pm 6.314$

Table 4: Calculation of C. I.$_{90}$ on Dynamic Stabilities for each Type of Motion.

Motion	D. F.	Disk Number	$\psi\sqrt{s^2_{y.x}}$ 1/cm. Drop 1	Drop 2	Drop 3	x_1 Average	$\sum(x_{1_k} - x_1)^2$	$\sqrt{S^2_m}$	90% Confidence Intervals (8)
Stable	2	6	11.49	14.92	14.08	13.50	6.39	1.03	$10.49 \leqq x_1 \leqq 16.51$
Wave I-A	8	13	7.04	6.02	8.55	7.23	6.31	0.30	$6.68 \leqq x_1 \leqq 7.78$
		16	8.20	7.52	6.21				
		43	6.41	7.81	7.30				
Wave I-B	11	19	4.46	4.78	5.03	4.57	1.83	0.12	$4.36 \leqq x_1 \leqq 4.78$
		20	4.26	5.46	4.29				
		23	4.29	5.02	4.44				
		27	4.15	4.24	4.44				
Wave III	11	32	1.86	0.68	0.44	1.40	2.55	0.14	$1.15 \leqq x_1 \leqq 1.65$
		35	1.48	1.56	1.29				
		37	1.28	1.97	1.44				
		40	1.09	1.74	2.01				
Transition	-	9							
		30							
		45							
Insufficient Data	-	46							

D.F. = Degrees of Freedom

Table 5: Physical Characteristics of Disks.

Disk Number	Weight grams	Moment of Inertia (gm. mass - cm^2)10^5	Thickness cm.	Disk Diameter cm.	Core Diameter cm.	Disk Density gm./$cm.^3$
6	4.022	158	0.654	2.543	0.399	1.217
9	5.429	164	0.628	2.544	0.791	1.700
13	10.397	260	0.650	2.544	1.416	3.150
16	12.335	336	0.616	2.543	1.661	3.943
19	15.854	492	0.618	2.540	1.952	5.060
20	17.078	556	0.623	2.543	2.034	5.395
23	20.531	754	0.648	2.544	2.223	6.237
27	25.810	1154	0.650	2.540	2.540	7.843
30	22.113	1113	0.647	2.540	1.020	6.742
32	19.167	1034	0.636	2.541	1.341	5.950
35	15.835	921	0.627	2.540	1.646	4.986
37	14.186	864	0.645	2.540	1.822	4.341
40	10.703	677	0.635	2.538	2.067	3.333
43	7.210	452	0.639	2.539	2.306	2.230
45	5.425	319	0.639	2.542	2.421	1.674
46	4.016	206	0.634	2.542	2.503	1.250

Table 6: Average Times Required for Disks to Descend 100 cm. in Triethylene Glycol at Various Liquid Temperature.

Disk Number	Time in sec. 66°F One Drop	Time in sec. 86°F Avg. Two Drops	Time in sec. 88°F Avg. Three Drops	Time in sec. 89oF Avg. Three Drops	Time in sec. 90°F Avg. Three Drops
6	12.9	11.1	10.9	11.2	10.5
7	----	6.5	6.5	6.4	6.1
8	----	6.1	6.1	6.1	6.1
9	4.2	4.3	4.5	4.6	4.5
10	----	3.7	3.6	3.7	3.7
11	----	2.9	3.0	3.0	2.9
13	2.2	2.3	2.5	2.5	2.5
16	2.2	2.1	2.2	2.2	2.2
19	1.9	1.9	1.9	1.9	1.9
20	1.8	1.8	1.8	1.8	1.7
23	1.5	1.5	1.5	1.6	1.5
27	1.3	1.3	1.4	1.4	1.4
30	----	1.7	1.6	1.5	1.4
32	1.5	1.6	1.6	1.6	1.5
35	1.6	1.8	1.9	1.9	1.9
37	2.0	2.0	1.9	1.9	1.9
40	2.1	2.3	2.4	2.3	2.4
43	3.0	3.2	3.3	3.2	3.5
45	4.2	4.6	4.6	4.7	4.6
46	10.3	9.1	8.9	8.9	8.7

Table 7: Dynamic Stabilities and Other Pertinent Final Results For Drop Two in Triethylene Glycol at 88°F.

Disk Number	θ Frames Read	t_θ sec.	$\psi s^2_{y.x}$ $1/cm^2$	$\psi\sqrt{s^2_{y.x}}$ 1/cm.	ψ_{Area} 1/cm.	Re = $\frac{Dvp}{\mu}$	$Re_s = \frac{D_s vp}{\mu}$
6	182	9.96	131.54	11.49	16.38	109	80
9	73	3.99	18.08	4.26	5.49	264	193
13	40	2.20	49.48	7.04	10.17	476	347
16	35	1.95	66.94	8.20	12.82	541	395
19	30	1.65	19.85	4.46	6.74	626	457
20	29	1.66	18.05	4.26	6.46	661	482
23	26	1.33	18.39	4.29	6.98	793	579
27	22	1.21	17.23	4.15	6.06	850	620
30	25	1.49	17.75	4.22	6.67	744	543
32	27	1.55	3.44	1.86	2.63	744	543
35	23	1.33	2.18	1.48	1.90	626	457
37	25	1.35	1.64	1.28	1.75	626	457
40	24	1.46	1.18	1.09	1.63	496	362
43	54	2.90	41.21	6.41	8.68	360	263
45	71	4.08	18.89	4.35	5.98	259	189
46	—	—	—	—	—	—	—

t_θ = time required for particle to descend d_θ ft., or through θ frames.

D = diameter of disk.

D_s = diameter of sphere with same volume as disk.

Table 8: Dynamic Stabilities and Other Pertinent Final Results for Drop Two in Triethylene Glycol at 89°F.

Disk Number	θ Frames Read	t_θ sec.	$\psi_{s^2_{y.x}}$ 1/cm²	$\psi_{\sqrt{s^2_{y.x}}}$ 1/cm	ψ_{Area} 1/cm	$Re = \frac{Dv\rho}{\mu}$	$Re_s = \frac{D_s v\rho}{\mu}$
6	75	8.39	224.22	14.92	17.32	108	78
9	71	4.06	5.46	2.34	2.70	262	191
13	38	2.12	36.37	6.02	8.30	482	352
16	34	1.93	56.55	7.52	10.31	547	400
19	25	1.42	22.80	4.78	6.24	634	463
20	29	1.57	30.00	5.46	8.18	669	488
23	26	1.42	25.32	5.02	8.42	753	550
27	22	1.26	17.90	4.24	6.39	860	628
30	25	1.44	1.19	1.09	1.42	803	586
32	27	1.55	0.46	0.68	0.83	753	550
35	22	1.27	2.42	1.56	2.02	634	463
37	25	1.35	3.89	1.97	2.64	634	463
40	27	1.49	3.05	1.74	2.37	524	382
43	53	2.80	60.88	7.81	10.15	376	275
45	73	4.13	55.21	7.41	9.30	256	187
46	67	7.28	78.22	8.85	10.73	135	99

t_θ = time required for particle to descend d_θ ft., or through θ frames.

D = diameter of disk.

D_s = diameter of sphere with same volume as disk.

Table 9: Dynamic Stabilities and Other Pertinent Final Results for Drop Three in Triethylene Glycol at 90°F.

Disk Number	θ Frames Read	t_θ sec.	$\psi\, s^2_{y.x}$ 1/cm^2	$\psi\sqrt{s^2_{y.x}}$ 1/cm	ψ Area 1/cm	$Re = \frac{Dv\rho}{\mu}$	$Re_s = \frac{D_s v\rho}{\mu}$
6	80	8.88	200.68	14.08	20.01	116	84
9	71	3.92	3.95	1.99	2.42	279	204
13	38	2.15	73.32	8.55	14.48	491	358
16	30	1.70	38.84	6.21	7.75	558	407
19	30	1.69	25.16	5.03	7.63	646	471
20	28	1.49	18.47	4.29	6.08	722	527
23	25	1.28	19.78	4.44	6.40	818	597
27	19	1.21	19.82	4.44	6.36	876	640
30	26	1.35	5.53	2.35	3.32	876	640
32	25	1.44	0.19	0.44	0.51	818	597
35	21	1.17	1.66	1.29	1.69	646	471
37	33	1.83	2.09	1.44	1.86	646	471
40	28	1.61	4.03	2.01	2.79	511	373
43	59	3.43	53.14	7.30	10.13	350	256
45	74	4.08	37.91	6.17	8.65	267	195
46	71	7.67	175.41	13.16	17.68	141	103

t_θ = time required for particle to descend d_θ ft., or through θ frames.

D = diameter of disk.

D_s = diameter of sphere with same volume as disk.

Table 10: Observations of diameter rotation on disks descending 100 cm. in triethylene glycol at 90° ± 3°F.

Disk Number	1	2	3	4	5
6	/	/	/	/	/
7	/	/	/	—	—
8	/	/	/	—	—
9	/	/	/	/	/
10	/	/	/	—	—
11	/	/	/	—	—
13	/	/	/	/	/
16	/	/	/	/	/
19	/	/	/	/	/
20	—	$X_{5°}$	/	/	/
23	/	$X_{10° - 15°}$	/	/	/
27	/	/	/	/	/
30	$X_{20°}$	/	/	/	/
32	/	—	/	/	/
35	/	/	/	/	/
37	$X_{20°}$	/	/	/	/
40	/	/	/	/	/
43	/	/	/	/	/
45	/	/	/	/	/
46	/	/	/	/	/

Top view of descending disk and corresponding designation in table.

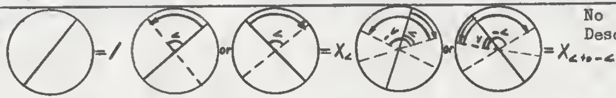

No Descent = —

Table 11: Observations of diameter rotation on disks descending 100 cm. in water at 80° ± 3°F.

Disk Number	1	2	3	4	5
1	X_{45°	X_{45°	X_{75°	X_{70°	X_{15°
6	X_{45°	X_{60°	X_{100°	X_{70°	X_{15°
9	X_{90°	X_{180°	X_{5° to − 200°	X_{200°	X_{50°
13	/	/	X_{90° near bottom	X_{80° near bottom	/
16	X_{20°	X_{40°	X_{50° near bottom	X_{60°	X_{10°
19	X_{60°	X_{10° to − 60°	/	X_{20° to − 10°	X_{20°
20	X_{5° to − 20°	X_{10° to − 20°	/	/	/
23	X_{15°	/	X_{45° near bottom	X_{20° to − 10° near bottom	X_{20°
27	X_{5°	/	/	/	/
30	/	—	/	/	/
32	/	/	/	/	/
35	/	—	X_{10°	X_{10°	X_{15°
37	/	X_{5° near bottom	/	/	/
40	/	X_{10° to − 10°	X_{10° to − 20°	X_{5° near bottom	X_{20°
43	X_{5° to − 25°	X_{40°	X_{5° near bottom	X_{5° near bottom	X_{10° to − 10°
45	X_{170°	X_{10° to − 180°	X_{200° near bottom	X_{100°	X_{10° to − 30°
46	X_{120°	X_{145°	X_{200° near bottom	X_{170°	/

Top view of descending disk and corresponding designation table.

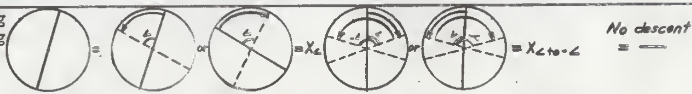

Table 12: Measured Angle or Angles Between Vertical Plane Through Path of Disk Descent and a Reference Vertical Plane in a 100 cm. Deep Triethylene Glycol Column at 90 ± 3° F.

Disk Number	Drop 1	Drop 2	Drop 3	Drop 4
6	----	----	----	----
9	-60°	-40°	15°	60°
13	85°	-60°	-55°	-60°
16	55°	-50°	-35°	50°
19	60°	-45°	-53°	55°
20	-40°	-45°	47°	50°
23	50°	65°	-70°	-60°
27	35°	75°	-70°	0°
30	80°	-70°	50°	90°
32	-50° to -80°	-85°	70°	-85°
35	50°	-65° to -80°	80°	50°
37	40°	65°	60°	90°
40	-80°	-85°	75°	-60°
43	-60°	-45°	-90°	-55°
45	----	70°	-85°	-80°
46	----	----	----	----

Table 13: Observed Motions of Disk Descending Approximately 100 cm. in Triethylene Glycol at 90±3°F.

Disk Number	Motion – Side View		
	Drop 1	Drop 2	Drop 3
6	Stable	Stable	Stable
9	Flutter	Wave	Flutter
13	Flutter	Wave	Wave
16	Small Wave	Wave	Wave
19	Wave	Wave	Wave with Flutter
20	Flutter	Wave	Wave with Flutter
23	Wave	Wave	Wave
27	Wave	Wave	Wave
30	Wave	Wave – Hit Wall	Wave with Flutter
32	Wave – Hit Wall	Wave – Hit Wall	Wave – Hit Wall
35	Wave – Hit Wall	Wave – Hit Wall	Wave – Hit Wall
37	Wave – Hit Wall	Wave – Hit Wall	Wave – Hit Wall
40	Wave – Hit Wall	Wave – Hit Wall	Wave – Hit Wall
43	Small Wave	Flutter	Wave
45	Small Wave	Small Wave	Flutter
46	Stable	Stable	Stable

Table 13 (Concl.):

Disk Number	Motion – Top View	
	Drop 4	Drop 5
6	Stable	Stable
9	Oscillation	Large Flutter
13	Wave with Oscillation w/o Diameter Rotation	Wave
16	Wave	Wave with Oscillation w/o Diameter Rotation
19	Wave	Wave
20	Wave	Wave
23	Wave	Wave
27	Wave	Wave
30	Wave	Wave
32	Wave – Hit Wall	Wave – Hit Wall
35	Wave – Hit Wall	Wave – Hit Wall
37	Wave – Hit Wall	Wave – Hit Wall
40	Wave – Hit Wall	Wave – Hit Wall
43	Small Wave	Large Flutter
45	Very Small Wave	Flutter and Oscillation w/o Diameter Rotation
46	Stable	Stable

Table 14: Observed motions of disk descending approximately 100 cm. in water at 80 $\pm$ 3^{o}F.

Disk Number	Combined Top and Side Views of Particle Motion		
	Drop 1	Drop 2	Drop 3
1	Spiral	Spiral	Spiral
6	Spiral	Oscillation with Diameter Rotation in Planar Wave	Spiral
9	Planar Wave to Spiral	Planar Wave with Diameter Rotation to Spiral	Spiral
13	Planar Wave to Spiral	Planar Flutter	Planar Wave to Spiral
16	Flutter or Small Planar Wave	Planar Flutter	Non-Planar Wave
19	Planar Wave	Small Planar Wave with Rotation Near Bottom	Small Planar Wave
20	Planar Wave to Spiral	Planar Flutter	Small Planar Wave
23	Completely Erratic	Planar Flutter	Small Planar Wave
27	Completely Erratic	Planar Flutter	Planar Wave - Hit Side
30	Hit Side Planar Wave	Planar Wave - Hit Side	Planar Wave - Hit Side
32	Hit Side Planar Wave	Hit Side Planar Wave	Hit Side Rolling Motion
35	Hit Side Planar Wave	Hit Side Completely Erratic	Hit Side Rolling Motion
37	Planar Wave	Planar Wave	Hit Side Rolling Motion
40	Planar Wave to Spiral to Planar Wave	Planar Wave	Planar Wave
43	Planar Wave to Spiral	Planar Wave to Spiral	Planar Wave
45	Planar Wave to Spiral	Planar Wave to Spiral	Planar Wave to Spiral
46	Planar Wave to Spiral	Planar Wave to Spiral	Planar Wave to Spiral

Table 14 (Concl.):

Disk Number	Top View of Particle Motion	
	Drop 2	Drop 3
1	Started Planar Oscillation To Spiral	Spiral
6	Oscillation with Diameter Rotation in Planar Wave	Planar Flutter to Non-Planar to Spiral
9	Non - Planar Wave	Planar Flutter to Spiral
13	Planar Flutter	Planar Flutter to Spiral
16	Flutter or Small Planar Wave	Planar Flutter
19	Planar Flutter	Planar Wave
20	Planar Flutter	Planar Wave
23	Planar Wave with Rotation of Plane Near Bottom	Planar Wave
27	Small Planar Wave	Planar Wave
30	Hit Side Rolling Motion	Planar Wave
32	Hit Side Small Planar Wave	Hit Side Rolling Motion
35	Hit Side Small Planar Wave	Hit Side Non - Planar Wave
37	Small Planar Wave	Hit Side Non - Planar Wave
40	Planar Wave	Planar Wave
43	Planar Wave to Spiral	Planar Wave
45	Planar Wave to Spiral	Planar Flutter to Spiral
46	Planar Wave to Spiral	Planar Flutter to Spiral

Table 15: Observations Obtained from Sketches of Movies and Movies of Disk Descents in Triethylene Glycol at 90° ± 3°F.

Disk Number	Motion		
	Drop 1	Drop 2	Drop 3
6	Stable	Stable	Stable
9	Wave I	Wave I	Wave I
13	Wave I	Wave I	Wave I
16	Wave I	Wave I	Wave I
19	Wave I (I-B)	Wave I (I-B)	Wave I ——
20	Wave I (I-B)	Wave I (I-B)	Wave I ——
23	Wave I (I-B)	Wave I (I-B)	Wave I ——
27	Wave I (I-B)	Wave I (I-B)	Wave I ——
30	Wave I (I-B)	Wave III	Wave III
32	Wave III	Wave III	Wave III
35	Wave III	Wave III	Wave III
37	Wave III	Wave III	Wave III
40	Wave III	Wave III	Wave III
43	Wave I	Wave I	Wave I
45	Wave I	Wave I	Wave I
46	Stable	Stable	Stable

Triethylene Glycol as the Fluid Media

Triethylene Glycol was a relatively new compound commercially at the initiation of this reeearch. Its high boiling point, low volatility, low toxicity, low corrosion rate, and high stability made it ideal as a high boiling eolvent. These same properties plus its high viscosity at room temperatures and its transparency made it similarly ideal for the etudy of particle motione. Theee propertiee are presented in tables and graphs published in Dow Glycols (2).

Because of the hygroscopio property of glycols, it was imperative to determine whether changes in the water content of the fluid media had occurred between the times of utilization of the fluid media. As an example, an evaluation of the viscosity of the fluid media required the determination of a deneity value by actual measurement. This, in turn, provided a step toward the determination of the percentage of pure triethylene glycol in the fluid media. The density of the fluid media was obtained by the utilization of a volumetric flask, scales, and a properly seleoted eample. From thie density and the density of pure water at the eame temperature, 25°C, the specific gravity of the fluid media at 25°C was calculated, With this information the percentage of Triethylene Glycol was found from a plot of specific gravity, 25°C/25°C, versus per cent glycol by weight (2). In turn the viscosity at any desired temperature wae found from a plot of absolute viscositiee of aqeous Triethylene Glycol solutions versue Temperature (2). It was found that over a twelve month period with the proper protection of the fluid from the atmosphere no appreoiable change occurred in the water content of the approximately 200 lbs. of fluid. It remained approximately 100% pure Triethylene Glycol.

TABLE OF NOMENCLATURE

1. $s^2_{y \cdot x}$ = mean square deviation from regression.

2. $s_{y \cdot x}$ = sample standard deviation from regrsssion = $\sqrt{s^2_{y \cdot x}}$.

3. $s^2_{y \cdot x\theta} = s^2_{y \cdot x}\ (F_\theta)$.

4. θ = number of motion picture frames through which disk is measured.

5. $\psi s^2_{y \cdot x}$ = dynamic stability bassd on $s^2_{y \cdot x} = \frac{1}{s^2_{y \cdot x}}$.

6. $\psi\sqrt{s^2_{y \cdot x}}$ = dynamic stability = $\sqrt{\psi s^2_{y \cdot x}}$.

7. ψ_{AREA} = dynamic stability based on area between least squares curvs and path of disk dsscent, per unit time.

8. ψ' = dynamic unstability, $\frac{1}{\psi s^2_{y \cdot x}}$, $\frac{1}{\psi s^2_{y \cdot x}}$, or $\frac{1}{\psi_{AREA}}$.

9. $d_{y \cdot x}$ = absolute deviations from regression = sy.x (θ-2).

10. t_{100} = time required for disk to descend 100 cm.

11. t_θ = time requirsd for disk to descend θ framss.

12. L_H = measured height of top reference line, relativs to bass lins.

13. L_P = msasursd height of disk, relative to base line.

14. L_L = measured hsight of bottom reference line, relative to base line.

15. T.L. = $\frac{100}{L_H - L_L}$ = factor for adjusting relative values to trus values.

16. $h_i = (L_P - L_L)\ \left(\frac{100}{L_H - L_L}\right)$ = true height of particls abovs refersnce line.

17. n = number of sample undsr statistical considsration.

18. k = y interospt of lsast squares line.

19. j = slope of lsast squares line.

20. I = moment of inertia of disk.

TABLE OF NOMENCLATURE (concl.)

21. Re = Reynolds number bassd on D = $\frac{DV\rho}{\mu}$.

22. D = diameter of disk in feet.

23. V = average velocity of disk in feet per second.

24. ρ = density of disk in pounds/feet cube.

25. μ = viscosity in British viscosity units.

26. Re_s = Reynolds number based on $D_s = \frac{D_s V\rho}{\mu}$.

27. D_s = diameter of sphere having sams volume as disk.

28. $t_{0.05}$ = student's t for 95 per cent confidsnce interval = 2.571.

29. F = conversion factor of framss to seconds.

30. x = time axis
31. y = height axis

$\left.\begin{array}{l} \text{30. } x = \text{time axis} \\ \text{31. } y = \text{height axis} \end{array}\right\}$ on plot of disk path (PLATE XIV).

TABLE OF DEFINITIONS

1. Drop referred to a sum of single descents for all disks investigated.
2. Descent referred to a movement downward of a single disk.
3. Dynamic stability referred to the stability of a disk during free fall in a container of infinite proportions.
4. Parallax was defined as a distortion of the measured values of the differences between consecutive positions of a descending disk.
5. Consecutive positions referred to consecutive frames on the film of the descent of a disk where these positions, or frames, were separated by a constant time increment.
6. Confidence intervals were defined as the limits between which a true value had a certain probability of existing.
7. Dark room was the room containing the equipment for measuring disk heights on the films of the descent.
8. Least squares line was the best possible straight line through a plot of the path of the particle descent which minimizes the squares of the deviations.
9. Measuring error referred to the error resulting from the measurements of disk height made on the films of the disk descent.
10. Extraneous disturbances referred to disturbances caused by movements outside of the measuring area.
11. Stable Motion (See PLATE XVII).
12. Wave I (See PLATE XVII).
13. Wave II (See PLATE XVIII)
14. Wave III (See PLATE XVIII).

TABLE OF DEFINITIONS (concl.)

15. Oscillation (See PLATE XVIV).

16. Spiral (See PLATE XVIV).

17. Agile plastic stars were star shaped pieces of plastic approximately $1\frac{1}{2}$ inches in diameter and $\frac{1}{2}$ inch thick used normally to minimize evaporation from a liquid surface.

18. Moment of Inertia referred to integral from center of the core to outside of the core of the differential mass times the arm squared plus integral from outside of core to outside of rim of the differential mass times arm squared, where the arm is the distance from the center of the disk to each differential mass.

IBM 650 PROGRAMS

for

COMPUTATION OF DYNAMIC STABILITY

SOAP

Output

Of A

FORTRANSIT

Program

For

$\psi s^2_{y.x}$ And Least Squares Line

Programmed

by

Mr. Thomas L. Hamilton

IBM 650

Kansas State University

Program is preceded by a SOAP package deck from FORTRANSIT II.

```
        REG   Y0002      0054           0000   00  0000  0000
E00BT   STO   EXITT                     0104   24  0057  0060
        NZU              EXITT          0060   44  0063  0057
        STU   SIGNS                     0063   21  0068  0071
        RAM    8003                     0071   67  8003  0079
        RAU    8002                     0079   60  8002  U087
        SRT    0002                     0087   30  0002  0093
        STU   COUNT                     0093   21  0098  0001
        RSL    8002                     0001   66  8002  0059
        ALO   PHPHI                     0059   15  0062  0067
        SRT    0004                     0067   30  0004  0077
        ALO              SKIPS          0077   15  0080  0085
        SRT    0000      TRIES          0080   30  0000  0103
SKIPS   STL   TEMPO                     0085   20  0089  0092
        RAU   COUNT                     0092   60  0098  0153
        SLT    0002      TEMPO          0153   35  0002  0089
TRIES   STU   COUNT                     0103   21  0098  0101
        RAU   SIGNS                     0101   60  0068  0073
        BMI              POSIT          0073   46  0076  0127
        RSU   COUNT      EXITT          0076   61  0098  0057
POSIT   RAU   COUNT      EXITT          0127   60  0098  0057
PHPHI    55    0000       0000          0062   55  0000  0000
E00SU   STO   EXITT                     0154   24  0057  0110
        NZU              EXITT          0110   44  0113  0057
        STU   SIGNS                     0113   21  0118  0121
        RAM    8003                     0121   67  8003  0129
        RAU    8002                     0129   60  8002  0137
        SCT    0000                     0137   36  0000  0109
        AUP   FIFIV                     0109   10  0112  0117
        SUP    8002                     0117   11  8002  0075
        STU   ABSOL                     0075   21  0130  0083
        RAU   SIGNS                     0083   60  0118  0123
        BMI              PLUSS          0123   46  0126  0177
        RSU   ABSOL      EXITT          0126   61  0130  0057
PLUSS   RAU   ARSOL      EXITT          0177   60  0130  0057
FIFIV    00    0000       0060          0112   00  0000  0060
1  SQU  ARE    ROOT      SUBRO  U       0000   00  0000  0060
E00AU   STO   SEXT                      0204   24  0107  0160
        BMI   SERR                      0160   46  0163  0064
        NZE              SEXT           0064   45  0168  0107
        STU   SA                        0168   21  0072  0125
        FAO   S10                       0125   32  0078  0055
        FMP   SHAF       SB             0055   39  0058  0108
SB      STU   SSAV       SAB            0108   21  0162  0065
SAB     RAU   SA                        0065   60  0072  0227
        FOV   SSAV                      0227   34  0162  0212
        FAO   SSAV                      0212   32  0162  0139
        FMP   SHAF                      0139   39  0058  0158
        FSB   SSAV                      0158   33  0162  0189
        NZU              SR             0189   44  0143  0094
        BMI              SR             0143   46  0096  0094
        FAO   SSAV                      0096   32  0162  0239
        STU   SSAV       SAB            0239   21  0162  0065
SR      RAU   SSAV       SEXT           0094   60  0162  0107
SERR    HLT    0000      SEXT           0163   01  0000  0107
SHAF     50    0000       0050          0058   50  0000  0050
S10      10    0000       0051          0078   10  0000  0051
ES001    00    0000      LAAAA          0000   00  0000  0001
LAAAA   RAL   EZ001                     1999   65  0102  0157
        STL   W0002                     0157   20  1968  0171
        RAL   EZ002                     0171   65  0074  0179
        STL   W0003                     0179   20  1969  0122
        RAL   EZ003                     0122   65  0175  0229
        STL   W0004                     0229   20  1970  0173
        RAL   EZ004                     0173   65  0176  0081
        STL   W0005                     0081   20  1971  0124
        RAL   EZ005                     0124   65  0277  0131
        STL   W0006                     0131   20  1972  0225
        RAL   EZ006                     0225   65  0128  0133
        LOO   LABAA      E00AQ          0133   69  0086  1913
ES002    00    0000      LAHAA          0000   00  0000  0002
LABAA   RAU   EZ007                     0086   60  0289  0193
        STU   Y0027      LACAA          0193   21  0028  0181
ES003    00    0000      LACAA          0000   00  0000  0003
LACAA   RAU   EZ007                     0181   60  0289  0243
        STU   Y0028      LAOAA          0243   21  0029  0082
ES004    00    0000      LAOAA          0000   00  0000  0004
LAOAA   RAU   EZ007                     0082   60  0289  0293
        STU   Y0029      LAEAA          0293   21  0030  0183
ES005    00    0000      LAEAA          0000   00  0000  0005
LAEAA   RAU   EZ007                     0183   60  0289  0343
        STU   Y0030      LAFAA          0343   21  0031  0084
ES006    00    0000      LAFAA          0000   00  0000  0006
LAFAA   RAU   EZ007                     0084   60  0289  0393
        STU   Y0031      LAGAA          0393   21  0032  0135
ES007    00    0000      LAGAA          0000   00  0000  0007
LAGAA   RAA   Y0000                     0135   80  0001  0091
        LOO    8005                     0091   69  8005  0097
        STD   Y0032      LAHAA          0097   24  0033  0136
ET033    00    0000      LAHAA          0000   00  0100  U303
ES008    00    0000      LAHAA          0000   00  0000  0008
LAHAA   RAB   Y0000                     0136   82  0001  0142
```

```
        LOO    8006                   0142   69 8006 0148
        STO   Y0033   LAIAA           0148   24 0034 0187
ET038    00    0000   LAIAA           0000   00 0100 0308
ES009    00    0000   LAIAA           0000   00 0000 0009
LAIAA   RAL   EZ008                   0187   65 0090 0095
        STL   W0002                   0095   20 1968 0221
        RAL   EZ009                   0221   65 0174 0279
        LDD   LAJAA   E00AQ           0279   69 0132 1913
ES010    00    0000   LAJAA           0000   00 0000 0100
LAJAA   RAC   Y0000                   0132   88 0001 0088
        LOO    8007                   0088   69 8007 0144
        STO   Y0034   LAKAA           0144   24 0035 0138
ET048    00    0000   LAKAA           0000   00 0100 0408
ES011    00    0000   LAKAA           0000   00 0000 0101
LAKAA   RAU    6019                   0138   60 6019 0329
        STU   Y0035   LALAA           0329   21 0036 0339
ES012    00    0000   LALAA           0000   00 0000 0102
LALAA   RAU   Y0035                   0339   60 0036 0141
        STU   ACC                     0141   21 0000 0203
        RAL    8006                   0203   65 8006 0061
        STL   W0001                   0061   20 1967 0070
        RAU    8007                   0070   60 8007 0327
        MPY   EZ011                   0327   19 0180 0100
        ALO   W0001                   0100   15 1967 0271
        STL   W0001                   0271   20 1967 0120
        RSL   EZ011                   0120   66 0180 0185
        ALO   W0001                   0185   15 1967 0321
        SLT   Y0003                   0321   35 0004 0231
        ALO   LALAN                   0231   15 0134 0389
        LOO   ACC      8002           0389   69 0000 8002
LALAN   STO   Y0000   LAMAA           0134   24 0001 0254
ES000    00    0000   LAMAA           0000   00 0000 0000
LAMAA   AXC   Y0000                   0254   58 0001 0210
        RSL    8007                   0210   66 8007 0167
        STD   Y0034                   0167   24 0035 0188
        ALO   EZ010                   0188   15 0191 0145
        8MI   LANAA   ET048           0145   46 0198 0138
E8000    00    0000   LANAA           0000   00 0000 0000
LANAA   AXB   Y0000                   0198   52 0001 0304
        RSL    8006                   0304   66 8006 0111
        STD   Y0033                   0111   24 0034 0237
        ALO   Y0025                   0237   15 0026 0281
        8MI   LAOAA   ET038           0281   46 0184 0187
E8013    00    0000   LAOAA           0000   00 0000 0103
LAOAA   RAU   EZ007                   0184   60 0289 0443
        STU   Y0036   LAPAA           0443   21 0037 0140
E8014    00    0000   LAPAA           0000   00 0000 0104
LAPAA   RAU   EZ007                   0140   60 0289 0493
        STU   Y0037   LAQAA           0493   21 0038 0241
E8015    00    0000   LAQAA           0000   00 0000 0105
LAQAA   RA8   Y0000                   0241   82 0001 0147
        LOO    8006                   0147   69 8006 0253
        STO   Y0033   LARAA           0253   24 0034 0287
ET091    00    0000   LARAA           0000   00 0100 0901
ES016    00    0000   LARAA           0000   00 0000 0106
LARAA   RSU    4013                   0287   61 4013 0217
        FAO    4001                   0217   32 4001 0377
        STU   W0001                   0377   21 1967 0170
        RSU    4013                   0170   61 4013 0267
        FAO    4007                   0267   32 4007 0233
        FMP   EZ012                   0233   39 0186 0236
        FOV   W0001                   0236   34 1967 0317
        LOO           E00AA           0317   69 0220 1700
        STU   Y0038   LASAA           0220   21 0039 0192
E8017    00    0000   LASAA           0000   00 0000 0107
LASAA   RAU   Y0038                   0192   60 0039 0543
        FAO   Y0036                   0543   32 0037 0213
        LOO           E00AA           0213   69 0066 1700
        8TU   Y0036   LATAA           0066   21 0037 0190
E8018    00    0000   LATAA           0000   00 0000 0108
LATAA   RAU   Y0038                   0190   60 0039 0593
        FMP   Y0038                   0593   39 0039 0439
        FAD   Y0037                   0439   32 0038 0115
        LDD           E00AA           0115   69 0218 1700
        STU   Y0037   LAUAA           0218   21 0038 0291
E8000    00    0000   LAUAA           0000   00 0000 0000
LAUAA   AX8   Y0000                   0291   52 0001 0197
        R8L    8006                   0197   66 8006 0105
        8TD   Y0033                   0105   24 0034 0337
        ALO   Y0025                   0337   15 0026 0331
        BMI   LAVAA   ET091           0331   46 0234 0287
ES019    00    0000   LAVAA           0000   00 0000 0109
LAVAA   R8U   EZ013   LAVAO           0234   61 0387 0341
LAVAB   RAL   Y0025                   0354   65 0026 0381
        LOO   LAVAE   E00AE           0381   69 0284 1926
LAVAU   STU   ACC     LAVA8           0341   21 0000 0354
LAVAE   FAO   ACC                     0284   32 0000 0427
        STU   W0001                   0427   21 1967 0270
        RAL   Y0025                   0270   65 0026 0431
        STL   W0004                   0431   20 1970 0273
        RAL   EZ014   LAVAK           0273   65 0276 0481
```

```
LAVAJ   RAU  Y0036   LAVAL        0404   60  0037  0391
LAVAK   STL  ACC     LAVAJ        0481   20  0000  0404
LAVAL   LOD          E00AL        0391   69  0194  1850
        STU  ACC                  0194   21  0000  0303
        RAL  W0004                0303   65  1970  0275
        LDU          E00AE        0275   69  0178  1926
        STU  W0004                0178   21  1970  0323
        RAU  ACC                  0323   60  0000  0155
        FOV  W0004                0155   34  1970  0320
        RSU   8003                0320   61  8003  0477
        FAD  Y0037                0477   32  0038  0165
        FOV  W0001                0165   34  1967  0367
        LDD          E00AA        0367   69  0370  1700
        STU  Y0039   LAWAA        0370   21  0040  0643
ES020    00   0000   LAWAA        0000   00  0000  0200
LAWAA   RAL  Y0025   LAWAC        0643   65  0026  0531
LAWAB   RAU  Y0039   LAWAU        0454   60  0040  0195
LAWAC   LDD  LAWAB   E00AF        0531   69  0454  1752
LAWAU   FOV  ACC                  0195   34  0000  0150
        LOD          E00AU        0150   69  0353  0204
        LDO          E00AA        0353   69  0056  1700
        STU  Y0040   LAXAA        0056   21  0041  0244
ES021    00   0000   LAXAA        0000   00  0000  0201
LAXAA   RAL  Y0025   LAXAC        0244   65  0026  0581
LAXAR   RAU  Y0036   LAXAD        0504   60  0037  0441
LAXAC   LOD  LAXAB   E00AF        0581   69  0504  1752
LAXAU   FDV  ACC                  0441   34  0000  0200
        LDD          E00AA        0200   69  0403  1700
        STU  Y0041   LAYAA        0403   21  0042  0245
ES022    00   0000   LAYAA        0000   00  0000  0202
LAYAA   RAU  Y0040                0245   60  0041  0295
        FMP  Y0026                0295   39  0027  0527
        FAD  Y0041                0527   32  0042  0069
        LDD          E00AA        0069   69  0172  1700
        STU  Y0042   LAZAA        0172   21  0043  0146
EB023    00   0000   LAZAA        0000   00  0000  0203
LAZAA   RAU  Y0040                0146   60  0041  0345
        FMP  Y0026                0345   39  0027  0577
        RSU   8003                0577   61  8003  0235
        FAO  Y0041                0235   32  0042  0119
        LOO          E00AA        0119   69  0222  1700
        STU  Y0043   LBAAA        0222   21  0044  0247
ES024    00   0000   LBAAA        0000   00  0000  0204
LBAAA   RAL   8005                0247   65  8005  0205
        LOO          E00AF        0205   69  0208  1752
        STU  Y0044   LBHAA        0208   21  0045  0248
ES025    00   0000   LBHAA        0000   00  0000  0205
LBBAA   RAU  Y0044                0248   60  0045  0099
        FAD  Y0027                0099   32  0028  0255
        LDD          E00AA        0255   69  0258  1700
        STU  Y0027   LBCAA        0258   21  0028  0631
ES026    00   0000   LBCAA        0000   00  0000  0206
LBCAA   RAU  Y0044                0631   60  0045  0149
        FMP  Y0044                0149   39  0045  0395
        FAO  Y0028                0395   32  0029  0305
        LOO          E00AA        0305   69  0308  1700
        STU  Y0028   LBOAA        0308   21  0029  0182
ES027    00   0000   LBOAA        0000   00  0000  0207
LBDAA   RAU  Y0041                0182   60  0042  0297
        FAD  Y0029                0297   32  0030  0207
        LOD          E00AA        0207   69  0260  1700
        STU  Y0029   LBEAA        0260   21  0030  0283
ES028    00   0000   LBEAA        0000   00  0000  0208
LBEAA   RAU  Y0041                0283   60  0042  0347
        FMP  Y0041                0347   39  0042  0242
        FAO  Y0030                0242   32  0031  0257
        LOD          E00AA        0257   69  0310  1700
        STU  Y0030   ES029        0310   21  0031  0199
ES029    00   0000   LBGAA        0000   00  0000  0209
LBGAA   RAU  Y0041                0199   60  0042  0447
        FMP  Y0044                0447   39  0045  0445
        FAO  Y0031                0445   32  0032  0159
        LOD          E00AA        0159   69  0262  1700
        STU  Y0031   LBHAA        0262   21  0032  0334
EB030    00   0000   LBHAA        0000   00  0000  0300
LBHAA   RAU  Y0042                0334   60  0043  0497
        LOD          E00BT        0497   69  0503  0104
        BTU  Y0045   LBIAA        0503   21  0046  0249
EB031    00   0000   LBIAA        0000   00  0000  0301
LBIAA   RAU  Y0043                0249   60  0044  0299
        LDD          E00BT        0299   69  0355  0104
        STU  Y0046                0355   21  0047  0350
        RAU  Y0041                0350   60  0042  1503
        LOD          E00BT        1503   69  1521  0104
        STU  Y0041   LBJAA        1521   21  0042  1529
LBJAA   RAL  EZ001                1529   65  0102  0307
        BTL  W0002                0307   20  1968  1513
        RAL  EZ026                1513   65  0675  1511
        STL  W0003                1511   20  1969  0371
        RAL  EZ015                0371   65  0224  0379
        STL  W0004                0379   20  1970  0272
        RAL  EZ016                0272   65  0325  0429
```

```
          STL  W0005                        0429  20 1971 0373
          RAL  EZ017                        0373  65 0326 0681
          STL  W0006                        0681  20 1972 0274
          RAL  EZ004                        0274  65 0176 0731
          STL  W0007                        0731  20 1973 0375
          RAL  EZ005                        0375  65 0277 0781
          STL  W0008                        0781  20 1974 0376
          RAL  EZ018                        0376  65 0479 0333
          LDD  LBKAA  E00AR                 0333  69 0286 1907
ES000      00   0000  LBKAA                 0000  00 0000 0000
LBKAA     AXA  Y0000                        0286  50 0001 0292
          RSL   8005                        0292  66 8005 0349
          STD  Y0032                        0349  24 0033 0336
          ALO  Y0024                        0336  15 0025 0529
          BMI  LBLAA  ET033                 0529  46 0232 0136
ES033      00   0000  LBLAA                 0000  00 0000 0303
LBLAA     RAL  Y0024                        0232  65 0025 0579
          STL  W0001                        0579  20 1967 0420
          RAL  EZ014  LBLAE                 0420  65 0276 0831
LBLAD     RAU  Y0029  LBLAF                 0554  60 0030 0285
LBLAE     STL  ACC    LBLAD                 0831  20 0000 0554
LBLAF     LDD         E00AL                 0285  69 0238 1850
          STU  ACC                          0238  21 0000 0553
          RAL  W0001                        0553  65 1967 0421
          LDD         E00AE                 0421  69 0324 1926
          STU  W0001                        0324  21 1967 0470
          RAU  ACC                          0470  60 0000 0405
          FDV  W0001                        0405  34 1967 0417
          RSU   8003                        0417  61 8003 0425
          FAD  Y0030                        0425  32 0031 0357
          LDD         E00AA                 0357  69 0360 1700
          STU  Y0030  LBMAA                 0360  21 0031 0384
ES034      00   0000  LBMAA                 0000  00 0000 0304
LBMAA     RAL  Y0024                        0384  65 0025 0629
          STL  W0001                        0629  20 1967 0520
          RAL  EZ014  LBMAE                 0520  65 0276 0881
LBMAD     RAU  Y0027  LBMAF                 0604  60 0028 0383
LBMAE     STL  ACC    LBMAD                 0881  20 0000 0604
LBMAF     LDD         E00AL                 0383  69 0386 1850
          STU  ACC                          0386  21 0000 0603
          RAL  W0001                        0603  65 1967 0471
          LDD         E00AE                 0471  69 0374 1926
          STU  W0001                        0374  21 1967 0570
          RAU  ACC                          0570  60 0000 0455
          FDV  W0001                        0455  34 1967 0467
          RSU   8003                        0467  61 8003 0475
          FAD  Y0028                        0475  32 0029 0505
          LDD         E00AA                 0505  69 0358 1700
          STU  Y0028  LBNAA                 0358  21 0029 0282
ES035      00   0000  LBNAA                 0000  00 0000 0305
LBNAA     RAL  Y0024                        0282  65 0025 0679
          STL  W0001                        0679  20 1967 0620
          RAU  Y0027                        0620  60 0028 0433
          FMP  Y0029                        0433  39 0030 0230
          STU  ACC                          0230  21 0000 0653
          RAL  W0001                        0653  65 1967 0521
          LDD         E00AE                 0521  69 0424 1926
          STU  W0001                        0424  21 1967 0670
          RAU  ACC                          0670  60 0000 0555
          FDV  W0001                        0555  34 1967 0517
          RSU   8003                        0517  61 8003 0525
          FAD  Y0031                        0525  32 0032 0209
          LDD         E00AA                 0209  69 0312 1700
          STU  Y0031  LBOAA                 0312  21 0032 0335
ES036      00   0000  LBOAA                 0000  00 0000 0306
LBOAA     RAU  Y0031                        0335  60 0032 0483
          FDV  Y0028                        0483  34 0029 0332
          LDD         E00AA                 0332  69 0385 1700
          STU  Y0047  LBPAA                 0385  21 0048 0151
ES037      00   0000  LBPAA                 0000  00 0000 0307
LBPAA     RAL  Y0024  LBPAC                 0151  65 0025 0729
LBPAB     RAU  Y0027  LBPAD                 0654  60 0028 0533
LBPAC     LDD  LBPAB  E00AF                 0729  69 0654 1752
LBPAD     FDV  ACC                          0533  34 0000 0400
          LDD         E00AA                 0400  69 0703 1700
          STU  Y0048  LBQAA                 0703  21 0049 0202
ES038      00   0000  LBQAA                 0000  00 0000 0308
LBQAA     RAL  Y0024  LBQAC                 0202  65 0025 0779
LBQAB     RAU  Y0029  LBQAD                 0704  60 0030 0435
LBQAC     LDD  LBQAB  E00AF                 0779  69 0704 1752
LBQAD     FDV  ACC                          0435  34 0000 0450
          LDD         E00AA                 0450  69 0753 1700
          STU  Y0049  LBRAA                 0753  21 0050 0803
ES039      00   0000  LBRAA                 0000  00 0000 0309
LBRAA     RAU  Y0048                        0803  60 0049 0853
          FMP  Y0047                        0853  39 0048 0298
          RSU   8003                        0298  61 8003 0605
          FAD  Y0049                        0605  32 0050 0627
          LDD         E00AA                 0627  69 0280 1700
          STU  Y0050  LBSAA                 0280  21 0051 0754
ES040      00   0000  LBSAA                 0000  00 0000 0400
LBSAA     RSU  EZ013  LBSAD                 0754  61 0387 0491
```

```
LBSAB   RAL  Y0024              0804  65  0025  0829
        LOO  LRSAE   E00AE      0829  69  0382  1926
LBSAD   STU  ACC     L8SAB      0491  21  0000  0804
LRSAE   FAO  ACC                0382  32  0000  0677
        STU  W0001              0677  21  1967  0720
        RAU  Y0031              0720  60  0032  0437
        FMP  Y0047              0437  39  0048  0348
        RSU   8003              0348  61  8003  0655
        FAO  Y0030              0655  32  0031  0407
        FDV  W0001              0407  34  1967  0567
        LOD          E00AA      0567  69  0770  1700
        STU  Y0051              0770  21  0052  1502
        RAU   0387              1502  60  03R7  1512
        FDV  Y0051              1512  34  0052  1520
        STU  Y0052   L8TAA      1520  21  0053  0705
ES042    00   0000   L8TAA      0000  00  0000  0402
L8TAA   RAU  Y0050              0705  60  0051  0755
        LOO          E008T      0755  69  0161  0104
        STU  Y0050   L8UAA      0161  21  0051  0854
E8043    00   0000   L8UAA      0000  00  0000  0403
L8UAA   RAU  Y0047              0854  60  0048  0903
        LOD          E008T      0903  69  0259  0104
        STU  Y0047   L8VAA      0259  21  0048  0201
ES044    00   0000   L8VAA      0000  00  0000  0404
L8VAA   RAU  Y0051              0201  60  0052  0457
        LOO          E008T      0457  69  0263  0104
        STU  Y0051   LBWAA      0263  21  0052  0805
ES045    00   0000   LBWAA      0000  00  0000  0405
LBWAA   RAU  Y0052              0805  60  0053  0507
        LOO          E008I      0507  69  0313  0104
        STU  Y0052   L8XAA      0313  21  0053  0156
ES046    00   0000   L8XAA      0000  00  0000  0406
L8XAA   RAL  EZ019              0156  65  0309  0363
        STL  W0002              0363  20  1968  0571
        RAL  EZ020              0571  65  0474  0879
        STL  W0003   .          0879  20  1969  0322
        RAL  EZ021              0322  65  0575  0929
        STL  W0004              0929  20  1970  0423
        RAL  EZ022              0423  65  0426  0931
        STL  W0005              0931  20  1971  0524
        RAL  EZ003              0524  65  0175  0979
        STL  W0006              0979  20  1972  0625
        RAL  EZ004              0625  65  0176  0981
        STL  W0007              0981  20  1973  0476
        RAL  EZ005              0476  65  0277  1031
        STL  W0008              1031  20  1974  0727
        RAL  EZ023              0727  65  0330  0485
        LOO  LBYAA   E00AR      0485  69  0288  1907
ES000    00   0000   L8YAA      0000  00  0000  0000
LBYAA   RAL  EZ024              0288  65  0541  0495
        BTL  W0002              0495  20  1968  0621
        RAL  EZ025              0621  65  0574  1029
        STL  W0003              1029  20  1969  0372
        RAL  EZ026              0372  65  0675  1079
        STL  W0004              1079  20  1970  0473
        RAL  EZ027              0473  65  0526  1081
        STL  W0005              1081  20  1971  0624
        RAL  EZ028              0624  65  0777  1131
        8TL  W0006              1131  20  1972  0725
        RAL  EZ029              0725  65  0228  0583
        STL  W0007              0583  20  1973  0576
        RAL  EZ030              0576  65  1129  0633
        STL  W0008              0633  20  1974  0827
        RAL  EZ031              0827  65  0380  0535
        LOO  L8ZAA   E00AR      0535  69  0338  1907
E8048    00   0000   L8ZAA      0000  00  0000  0408
LBZAA   NOP   8000    R000      0338  00  8000  8000
EZ031    00   0007    0000      0380  00  0007  0000
EZ030    00   0000    0027      1129  00  0000  0027
EZ029    00   0000    0044      0228  00  0000  0044
EZ028    00   0000    002H      0777  00  0000  0028
EZ027    00   0000    0029      0526  00  0000  0029
EZ026    00   0000    0041      0675  00  0000  0041
EZ025    00   0000    0030      0574  00  0000  0030
EZ024    00   0000    0031      0541  00  0000  0031
EZ023    00   0007    004h      0330  00  0007  0046
EZ022    00   0000    0050      0426  00  0000  0050
EZ021    00   0000    0047      0575  00  0000  0047
EZ020    00   0000    0051      0474  00  0000  0051
EZ019    00   0000    0052      0309  00  0000  0052
EZ018    00   0007    0032      0479  00  0007  0032
EZ017    00   0000    0032      0326  00  0000  0032
EZ016    00   0000    0045      0325  00  0000  0045
EZ015    00   0000    004h      0224  00  0000  0046
EZ014    00   0000    0002      0276  00  0000  0002
EZ013    10   0000    0051      0387  10  0000  0051
EZ012    10   0000    0053      0186  10  0000  0053
EZ011    00   0000    000.      0180  00  0000  0006
EZ010    00   0000    0003      0191  00  0000  0003
EZ009    00   0001    0009      0174  00  0001  0009
EZ008    00   0003    0019      0090  00  0003  0019
EZ007    00   0000    0000      0289  00  0000  0000
EZ006    00   0005    0001      0128  00  0005  0001
EZ005    00   0000    0022      0277  00  0000  0022
EZ004    00   0000    0023      0176  00  0000  0023
EZ003    00   0000    0024      0175  00  0000  0024
EZ002    00   0000    0025      0074  00  000U  0025
EZ001    00   0000    002n      0102  00  0000  0026
        8OP                     1991  00  0000  1999
```

SOAP

Program

for

ψAREA

Programmed

by

Dr. Thomas S. Parker

IBM 650

Kansas State University

```
1 HIMEB    FOR MULA      FOR      STABILITY    1    0000   00 0000 0000
1                                              2    0000   00 0000 0000
           BLR  0500     1999                  3    0000   00 0000 0000
           RCO  1951                           4    0323   70 1951 0001
           RAU  1954                           5    0001   60 1954 0009
           RAC  0001                           6    0009   88 0001 0015
           STL  SUM                            7    0015   20 0019 0022
           LDD  AYE      FLOPT                 8    0022   69 0025 0028
  FIFIV    00   0000     0055                  9    0000   00 0000 0055
  FPTWO    20   0000     0051                 10    0050   20 0000 0051
  FIFT3    00   0053     0000                 11    0100   00 0053 0000
  FLOPT    STD  TEMPZ                         12    0028   24 0031 0034
           BMI  NEG                           13    0034   46 0037 0038
           SCT  0000                          14    0038   36 0000 0011
           STL  INDEX                         15    0011   20 0065 0018
           RAL  8003                          16    0018   65 8003 0075
           SRT  0002                          17    0075   30 0002 0081
           SLT  0002                          18    0081   35 0002 0087
           ALO  FIFIV                         19    0087   15 0000 0005
           SLO  INDEX                         20    0005   16 0065 0069
           RAU  8002     TEMPZ                21    0069   60 8002 0031
  NEG      RSU  8003                          22    0037   61 8003 0045
           SCT  0000                          23    0045   36 0000 0017
           STL  INDEX                         24    0017   20 0065 0068
           RAL  8003                          25    0068   65 8003 0125
           SRT  0002                          26    0125   30 0002 0131
           SLT  0002                          27    0131   35 0002 0137
           ALO  FIFIV                         28    0137   15 0000 0055
           SLO  INDEX                         29    0055   16 0065 0119
           RSU  8002     TEMPZ                30    0119   61 8002 0031
  AYE      STU  AY                            31    0025   21 0030 0033
           RAU  1955                          32    0033   60 1955 0059
           LDD  BEE      FLOPT                33    0059   69 0012 0028
  BEE      STU  BE                            34    0012   21 0016 0169
           FAD  AY                            35    0169   32 0030 0007
           STU  ZE       REPET                36    0007   21 0062 0115
  REPET    RCO  1951                          37    0115   70 1951 0051
           RAU  1956                          38    0051   60 1956 0061
           LDD  ETA      FLOPT                39    0061   69 0014 0028
  ETA      FSB  ZE                            40    0014   33 0062 0039
           STU  ETA1                          41    0039   21 0044 0047
           BMC           DONOT                42    0047   49 0150 0101
           FMP  ETA0                          43    0150   39 0003 0053
           BMI  OPPOS                         44    0053   46 0006 0057
           RAU  ETA1                          45    0057   60 0044 0049
           FAD  ETA0                          46    0049   32 0003 0029
           FDV  FPTWO                         47    0029   34 0050 0200
           RAM  8003                          48    0200   67 8003 0107
           RAU  8002                          49    0107   60 8002 0165
           FAD  SUM                           50    0165   32 0019 0095
           STU  SUM      DONOT                51    0095   21 0019 0101
  OPPOS    RAU  ETA1                          52    0006   60 0044 0099
           FSB  ETA0                          53    0099   33 0003 0079
           STU  DIFF                          54    0079   21 0084 0187
           FDV  FPTWO                         55    0187   34 0050 0250
           RAM  8003                          56    0250   67 8003 0157
           RAU  8002                          57    0157   60 8002 0215
           FAD  SUM                           58    0215   32 0019 0145
           STU  SUM                           59    0145   21 0019 0072
           RAU  ETA1                          60    0072   60 0044 0149
           FMP  ETA0                          61    0149   39 0003 0103
           FDV  DIFF                          62    0103   34 0084 0134
           RAM  8003                          63    0134   67 8003 0041
           RSU  8002                          64    0041   61 8002 0199
           FAD  SUM                           65    0199   32 0019 0195
           STU  SUM      DONOT                66    0195   21 0019 0101
  DONOT    SXC  0002                          67    0101   59 0002 0207
           LDD  ETA1                          68    0207   69 0044 0097
           STD  ETA0                          69    0097   24 0003 0056
           RAU  ZE                            70    0056   60 0062 0067
           FAD  BE                            71    0067   32 0016 0043
           STU  ZE       REPET                72    0043   21 0062 0115
  UNFLO    RAU  SUM                           73    0300   60 0019 0023
           SRT  0002                          74    0023   30 0002 0129
           RAL  8002                          75    0129   65 8002 0237
           SRT  0004                          76    0237   30 0004 0147
           SLO  FIFT3                         77    0147   16 0100 0105
           BMI  NAGET                         78    0105   46 0008 0109
           LDD  SHIFT                         79    0109   69 0118 0265
           SDA  SHIFT                         80    0265   22 0112 0315
           RAL  SUM                           81    0315   65 0019 0073
           SRT  0002     SHIFT                82    0073   30 0002 0112
  SHIFT    SLT  0000     PUNCH                83    0112   35 0000 0035
  NAGET    RSL  8002                          84    0008   66 8002 0117
           LDD  SHOFT                         85    0117   69 0020 0123
           SDA  SHOFT                         86    0123   22 0020 0173
           RAL  SUM                           87    0173   65 0019 0223
           SRT  0002     SHOFT                88    0223   30 0002 0020
  SHOFT    SRT  0000     PUNCH                89    0020   30 0000 0035
  PUNCH    STL  1977                          90    0035   20 1977 0080
           PCH  1977                          91    0080   71 1977 0027
           HLT  1111     1111                 92    0027   01 1111 1111
```

EXPLANATION OF PLATE XXVI

Photograph of drop column, corresponding to drawing of drop column presented in Plate II.

PLATE XXVI

AN INTRODUCTION TO A NEW CONCEPT:
THE DYNAMIC STABILITY
OF
DISKS FREELY DESCENDING IN A FLUID MEDIA

by

BILLY LEE HIMES, SR.

B. S., Kansas State University of
Agriculture and Applied Science, 1958

AN ABSTRACT OF A THESIS

submitted in partial fulfillment of the

requirements for the degree

MASTER OF SCIENCE

Department of Chemical Engineering

KANSAS STATE UNIVERSITY
OF AGRICULTURE AND APPLIED SCIENCE

1960

ABSTRACT

This study pertained to the characteristics of the motions of particles falling freely in a fluid.

There were four objectives to this investigation. The first was to refine the mathematical definition of a property of motion of each particle as it freely descended in an infinite expanse of fluid. This property was to be named dynamic stability. The second objective was to actually measure the behavior of the motion of each particle and subsequently calculate values of dynamic stability. The third was to observe and define the type of motion exhibited by each particle falling freely in a fluid. The fourth was to correlate the results of two and three.

The dynamic stabilities were found by dropping a series of particles, one at a time, through a glass column containing triethylene glycol. The descending particles were filmed on moving pictures and, from the individual frames of this film, measurements were made of the heights of the particles at equal increments of time. From these measurements a least squares line was calculated for the path of each particle. The mean deviation of the actual path of the particle from the least squares line gave dynamic unstability; the reciprocal of this quantity was taken as dynamic stability.

These investigations were conducted with disks - approximately one inch in diameter, a quarter inch thick, and of various weights and moments of inertia - descending in triethylene glycol at 88 to 90°F at Reynolds number, based on D_s, ranging from 78 to 640.

It was found that a disk, in a free-fall descent through triethylene glycol, exhibited one of three postulated types of motion; i. e. stable,

wave I, and wave III. It was further postulated that wave I motion consisted of subtypes; wave I-A and wave I-B. The distinction between these subtypes was shown by a fluctuation in the values of dynamic stability.

A relationship was found between all the postulated types of motion in triethylene glycol and the dynamic stabilities, $\psi\sqrt{s^2_{y.x}}$. Disk 6, exhibiting stable motion, had dynamic stabilities between 11.49 to 14.92 reciprocal cm. Disks postulated as exhibiting wave I-A, I-B, and III motions had ranges of dynamic stabilities of 6.02 to 8.55 reciprocal cm., 4.15 to 5.46 reciprocal cm., and 0.44 to 2.01 reciprocal cm., respectively. Each range of dynamic stabilities, corresponding to a particular type of subtype of motion, was distinct and separate.

From a comparison of the physical properties of the disks with the types of motion assigned each disk it was found that a low dynamic stability was associated with a high moment of inertia relative to weight of the disk. From a comparison of Reynolds numbers for each disk with the types of motion it was found that a Reynolds number, based on D_s, of less than one hundred was associated with stable motion.

This study shows that dynamic stability of disks is measurable and therefore must exist. The measurable dynamic stabilities also may be utilized to predict the types of motion of disks descending in a fluid media.